

Evaluation of pre- and post-laser treatment effects of welds in maritime industry

Master of Science in Technology Thesis
Materials Engineering
Modern Industrial Materials
Department of Mechanical and Materials Engineering

Author:
Inka Väisänen

17.03.2025
Turku

The originality of this thesis has been checked in accordance with the University of Turku quality assurance system using Turnitin OriginalityCheck service.

Master's thesis

Subject: Materials Engineering

Author: Inka Väisänen

Title: Evaluating pre- and post-laser treatment effects on material properties of welds in maritime industry

Supervisors: Adjunct professor Heidi Piili, D.Sc. (Tech), Milica Todorović, D.Phil.

Advisors: Nikhil Kamboj, D.Sc. (Tech), Mohsen Amraei, PhD

Number of pages: 82 pages

Date: 17.03.2025

Corrosion heavily impacts maritime industry as it has very often welded structures, and they are the especially prone to the effects of corrosion. This may lead to mechanical failure, as the welds are vulnerable to the damage. Compared to conventional cleaning methods that are used in maritime industry, such as sand blasting or grinding, laser cleaning is a method where the laser beam removes dirt, oil or other unwanted component from surface without damaging the substrate material below it. Laser polishing can decrease the surface roughness as a post-process by melting the surface layer of the metal with a laser pulse. The melted metal smoothens with surface tension and hardens quickly to form an even surface.

The aim of this thesis is to research if the laser cleaning as a pre-processing method and laser polishing as a post-processing method are beneficial when welds in material EH36 are used in maritime industry. Laser polishing was also tested as a post-processing method for 316 L stainless steel manufactured by laser bed powder fusion method (PBF-LB/M).

The laser processes were executed with an IPG YLPN nanosecond pulsed fiber laser with a maximum average power of 100W. The wavelength is minimum 1055 nm and maximum 1075 nm (typically 1064 nm). The samples were first laser cleaned and conventionally cleaned with a cylindrical grinding setup, and then laser polished from the top and bottom sides of the weld. The PBF-LB/M samples were only laser polished. A Gamry instruments surface corrosion system and an Ivium electrochemical analyser were used to test and analyse the corrosion properties. The roughness values were obtained with Bruker Alicona Infinite Focus G6 along with the surface inspection.

The laser power was varied between 25 W – 100 W and the pulse width was varied between 25 – 100 ns. The best results for laser cleaning were achieved with the average power of 25 W and pulse width of 75 ns. The optimal parameters for laser polishing were with the average power of 75 W and pulse width of 25 ns. The process speed was 450 mm/s and the pulse frequency was set to 10 kHz for both laser processes. The number of treatment rounds were set to six.

From the results it can be concluded that visually the laser cleaning was successful when compared to the conventionally cleaned sample as no rust or oil can be seen in the microscopic images. The surface roughness of the laser cleaned sample was also reduced, when compared to the conventionally cleaned sample, as the areal average roughness S_a was decreased 36 %. When laser polishing was studied as post-treatment for welds, laser polishing improved the S_a 22 % compared to the laser cleaned sample. The corrosion rate was lowered in the laser polished sample 68 %, when compared to the laser cleaned sample. Laser polishing also improved the surface roughness of 316L as the S_a value lowered 66 % compared to the non-laser polished 316 L sample. Additionally, the corrosion rate was reduced in the laser polished 316 L PBF-LB/M sample, it was 31 % less than the non-laser polished sample.

As corrosion has such high impact on maritime industry, improving the materials is vital. The results in this thesis indicate that the laser cleaning is a reasonable option to conventional cleaning methods. Material surface could be modified with a laser to be more resistant to corrosion without any additional materials or coatings.

Key words: Laser polishing, Laser cleaning, Weld treatment, NV E36, Surface Roughness, Corrosion, Metal, Additive manufacturing, AM, Laser-based powder bed fusion, PBF-LB/M, Maritime industry

Acknowledgements

First, I would like to express my gratitude to my supervisor Heidi Piili for the counselling and guidance during this thesis. With her ideas and expertise this thesis was shaped into a coherent whole. I would also like to thank Nikhil Kamboj and Mohsen Amraei for their insightful thoughts and helpful discussions. A special thanks to Antti Salminen for introducing me to the topic and for the insightful discussions.

Thank you also to the entire MALAMA project, this thesis has been done as a part of Surface preparation of the surface to be painted in the Marine context (MALAMA, Maalatus ja maalattavan pinnan esivalmistelu laserilla marine-kontekstissa) project (A80056). The project is funded by the European Regional Development Fund (ERDF) and Satakuntaliitto as a part of Uudistuva ja osaava Suomi 2021–2027 - EU Programme for Regional and Structural Policy. The duration of the project is 1.5.2023-30.4.2025. The parties involved are Machine Engineering department in the technical faculty of the University of Turku and Pori unit of the Turku school of Economics. There are also multiple industrial partners involved in the project. The main goal for the project is to bring laser technology -based surface cleaning forward to ship building and packaging industry. This is done in such way, that the economic and environmental possibilities are brought out. The end result is to see an overview of the technologies available in the context of ship building and maritime industry especially from the environmental and economical viewpoint.

I would also like to thank Eter Tourunen and Kristina Tarson for their contributions and valuable help during the experiments and during the writing process. I would like to thank the entire DMS-team in the Mechanical Engineering department that have helped me during this process. I would especially like to thank Aki, Saeid and Ammar, I would not have got the results without your knowledge and expertise with the needed equipment.

A special thanks goes to EOS and Niklas Lind for providing the 316L samples and for the support during the whole writing process.

Lastly, I would like to thank my friends and family for the guidance and encouragement throughout the whole process. This thesis would not have been made into a reality without taking my mind off it once in a while. And let us not forget the emotional support dog Cava!

Table of Contents

Nomenclature

1	Introduction	1
2	Laser cleaning	6
2.1	Overview of laser cleaning	6
2.2	Research case studies about laser cleaning.....	10
3	Laser polishing	12
3.1	Overview of laser polishing.....	12
3.2	Research case studies about laser polishing	13
4	Overview of corrosion	15
5	Aim and purpose of experimental part.....	18
6	Experimental setup	20
6.1	Maritime industry EH36 steel	20
6.2	PBF-LB/M of 316L stainless steel	21
6.3	Hardware.....	23
7	Experimental procedure	29
7.1	Material preparation	29
7.2	Pre-treatment (Part 1).....	29
7.3	Post-treatment (Part 2a).....	32
7.4	Post-treatment of PBF-LB/M (Part 2b)	33
7.5	Testing and analysis (Part 3).....	33
8	Results and discussion	35
8.1	Pre-treatment (Part 1).....	35
8.2	Post-treatment (Part 2).....	45
8.3	Corrosion analysis (Part 3).....	55
8.4	Uncertainties	67
9	Conclusions	68

10 Further studies.....	71
References	72
Appendices	75

Nomenclature

Symbol	Explanation
E_{Corr}	Open circuit potential, unit
F	Laser fluence
I_{corr}	Corrosion current density
P_{ave}	Average laser beam power
P_{peak}	Laser pulse peak power
Ra	Average roughness measured from a line
Rz	Mean roughness distance from highest peak to lowest valley measured from a line
Sa	Average roughness measured from an area
Sz	Mean roughness distance from highest peak to lowest valley measured from an area

Abbreviations

AM	Additive manufacturing
CW	Continuous wave laser
PBF-LB/M	Laser based powder bed fusion of metals

1 Introduction

Over the past few decades, laser technology has advanced significantly, and it has been established as an important technology in multiple industries. [1] Laser processing technologies such as laser cutting, or have been created to solve engineering problems that were previously hardly possible. [2] Lasers are growing more interest because of the unique qualities they have to offer: efficiency, accuracy, and versatility to use in many different applications. [3]

One of the applications where laser processing has been widely used is surface treatment. [3] Clean surfaces are important aspects in engineering, since it affects the mechanical durability, reliability and especially in the maritime industry, the ability to resist corrosion [4]. That is why laser cleaning has been developed. Especially the removal of oil is necessary, since it has huge negative effects on for example coating processes such as painting or fabrication processes such as welding or shaping the material sheets. [5] Traditionally, the oils have been cleaned with sandblasting, by using chemicals or by sanding with sandpaper but these can create considerable amount of possibly harmful waste. [6]

Laser cleaning processing adds multiple advantages to processing, such as high speed, and a possibility for remote-control. The damage to the base material is decreased, when the parameters of laser processing can be set locally due to the controllability of a laser beam. One important advantage is also the fact that laser cleaning processing does not produce any secondary waste during the process, which makes it environmentally friendly as a process. [7],[8],[9]

Laser cleaning has a market size estimated at USD 722,38 million in 2024. It is expected to rise to USD 947,21 million by 2029. This would mean that industries are keen on transferring more towards laser technology [10]. That is also why it is crucial to study laser cleaning and the applications it could be used in. Maritime industry has a lot of different applications laser cleaning is applicable, but one of the main processes laser cleaning could replace is the pre-treatment process for welding or painting. [8]

A similar technology to laser cleaning is laser polishing or laser polishing. In the recent years laser polishing has steadily had a rising interest on polishing metal surfaces by melting a fine layer of metal on the surface. Compared to laser cleaning, the method does not remove material but relocates it to achieve a smooth finish. [11], [12], [13]

Marine industry has a significant issue with corrosion. It may cause cracking, abrasion and fatigue, which will cause considerable risks. These risks may lead to failures that affect the reliability of the equipment and structures. The corrosion affects all infrastructure that are in contact with marine environment, such as bridges, harbour structures but especially ships. Sea water is a particularly corrosive environment and a challenge in the industry. [14],[15], [16], [17], [18]

The corrosion does not only affect the lifetime of a structure, but also is costly, as damaged or failed parts need to be replaced. This may not be an easy task, as some parts can be in small spaces and other may be expensive in other ways, such as in shape or labour. [19]

One of the ways these costs and damages could be reduced is to use additive manufacturing (AM). This technique has multiple advantages, such as it can be used to create a more intricate shapes that traditional methods may not be able to do. This is not yet used widely in maritime industry, but it has a lot of potential. The AM method in this thesis is laser powder bed fusion of metals (PBF-LB/M). [19]

According to an impact analysis made by NACE international, corrosion world-wide has the cost of around 2,5 trillion USD, which is out of the global GDP roughly 3;4 %. [10] If effects of corrosion can be reduced, all aspects that are affected by corrosion, such as maintenance, material cost and damage control become more economically profitable. This is why it is essential to study this topic further. [20]

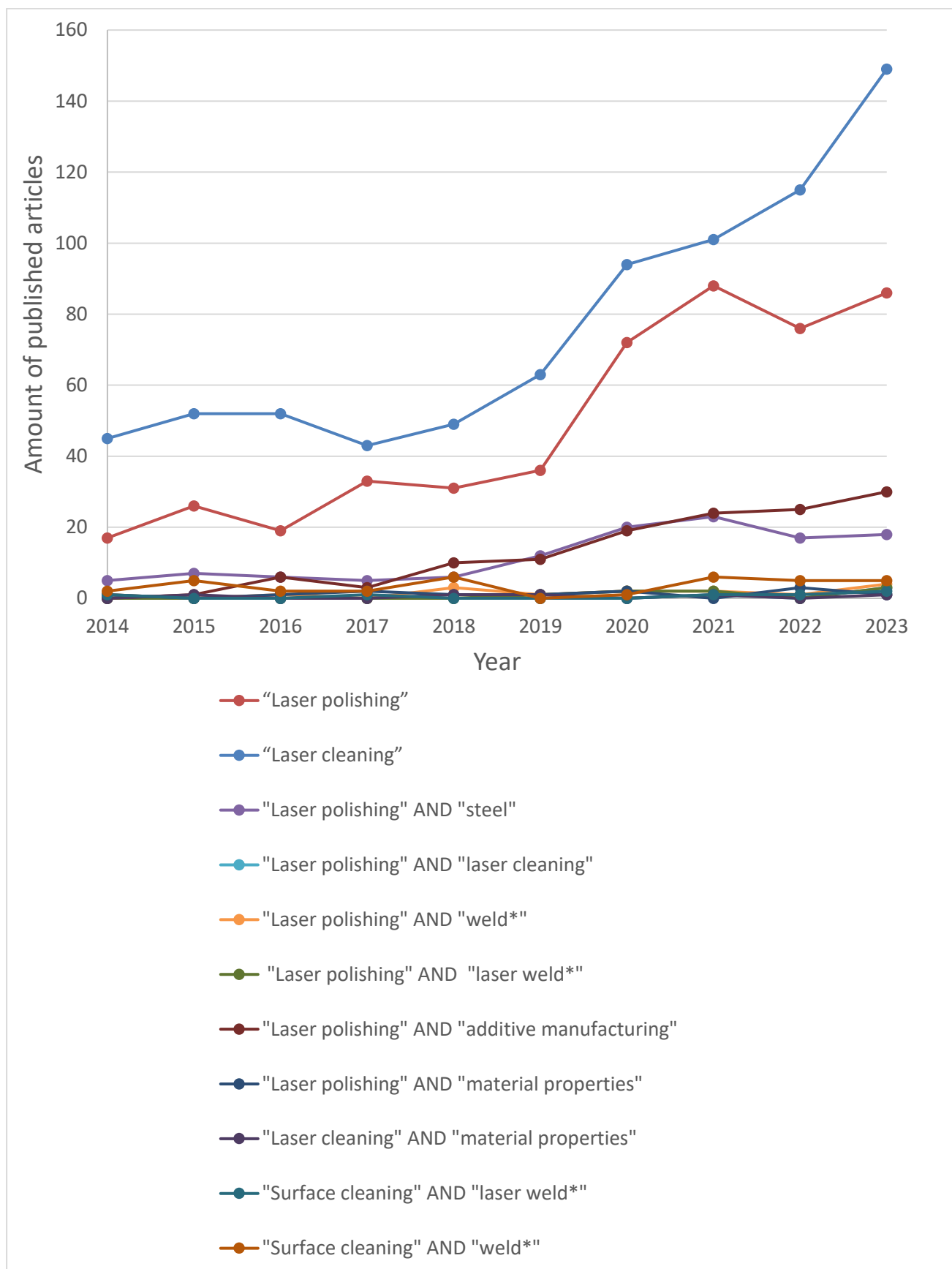


Figure 1. Number of publications per topic yearly according to Scopus with different key words.

As depicted in the Figure 1, the amount of publications has increased significantly in the last ten years with using keywords laser cleaning. Almost 150 publications were published in the year 2023. When compared to nine years prior, the amount was about 50. This means that from the past nine years there has been an improvement of 200 %. The second highest number of publications in 2023 was made about laser polishing, almost 90 publications. The most publications for laser polishing were published in the year 2021, then only six articles were published.

When laser polishing is combined with a search word weld, less than ten publications are published each year. It can be concluded that the topic is not widely researched yet. This can also be seen on this thesis, there is not a lot of literature that focuses on laser polishing a weld, which is why only a few articles are mentioned. When the weld is replaced with additive manufacturing, the number of publishes increases to about 30 in the year 2023. It is not a lot, but the amount has been increasing steadily from 2015. From this it can be concluded that the topic is not widely researched.

That is the motivation behind the thesis and one of the goals is to answer these research questions:

1. Is laser cleaning an effective way to clean a metal surface?
2. How can laser cleaning be compared to a conventional surface cleaning method in the case of welds?
3. Does laser polishing have an improving effect on the corrosion resistance of a weld?
4. How can the laser polishing of hot-rolled steel be compared to additively manufactured material?

The research questions can be seen in Figure 2 as a part of the whole thesis and motivation behind it.

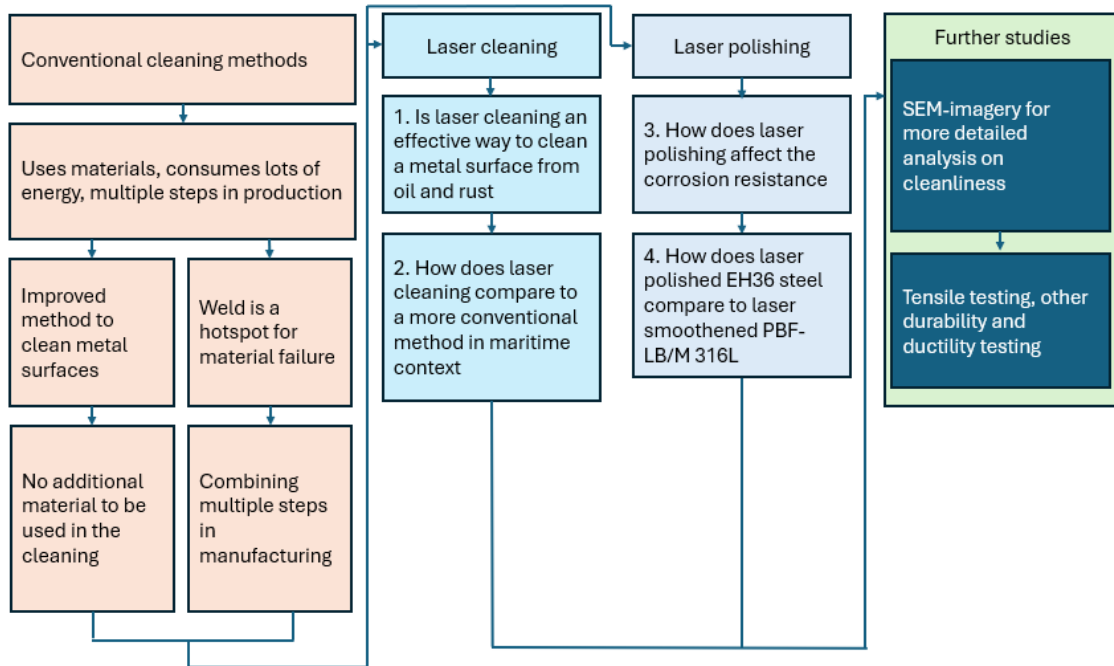


Figure 2. The scope and motivation for the thesis.

As shown in Figure 2, the first column has the motivation behind the thesis. The thesis questions are coloured as blue in the middle, and the third column is further studies that could be done based on the thesis. The motivation divides into two sides, what should be improved and what are some challenges right now, when conventional cleaning methods and welding is discussed. The research questions divide into two, the laser cleaning and laser polishing side. The further studies conclude what could be done to improve the results that were achieved in this thesis, as the topic is mainly limited to the pre- and post-processing of the welds. This is also why the topic of laser welding is not focused on this thesis.

This thesis has been made as a part of Surface preparation of the surface to be painted in the Marine context (MALAMA, Maalatun ja maalattavan pinnan esivalmistelu laserilla marine-kontekstissa). This has also motivated the thesis to be focused on the maritime industry.

2 Laser cleaning

2.1 Overview of laser cleaning

Laser cleaning is a process encompassing laser beam where the particles or hydrocarbons are removed from the top of a solid material, called as substrate. It is a non-contact laser interaction, in which a pulsed laser beam or a continuous wave laser beam can be applied [6].

The working principles of a pulsed laser beam and a constant wave laser beam differ a lot. A pulsed laser beam consists of multiple pulses with typical duration of milliseconds or less in between each pulse in a specific time period T . The principle of a pulsed laser can be seen in Figure 3.

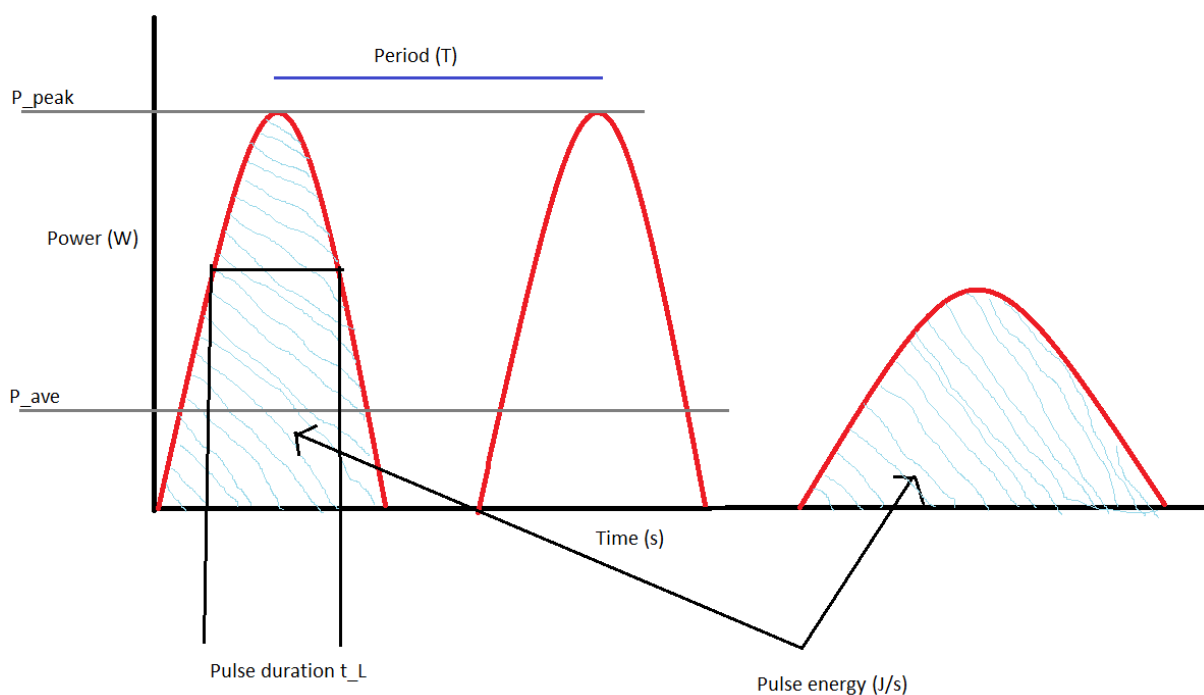


Figure 3. Pulsed laser mechanism in a power-time graph. Reproduced from [21] which is under an open access Creative Common CC BY license.

As can be seen from Figure 3, the pulses have peaks and a specific duration, that can be set before a process is started. The units of the peak power P_{peak} are watts, and the peak power is the highest power the pulse reaches during a pulse. Average power P_{ave} explains the total amount of watts per one pulse duration. Pulse duration, with the unit of seconds (s) sets the amount of time the pulse occurs. Pulse energy is the amount of energy in one pulse, which is called as period. The pulse energy emitted during one full period as a pulse is measured the

number of joules per second. Pulse energy can be used to measure the peak power, when the energy is divided by pulse duration. If all parameters, such as peak power, average power and pulse period stays the same, a shorter pulse duration gives out a higher peak power compared to a longer pulse duration t_L . [22] Another important parameter in laser processing is laser fluence F . It has the unit of J/mm^2 .

$$F = \frac{P_{laser}}{t_{pulse} * A}, \quad (1)$$

In the equation (1), P_{laser} is the laser pulse power, t_{pulse} is the pulse length and A is the beam cross-section area. All of the previously mentioned parameters can be changed according to the application and desired results. [23] Because of the pulses, there is a specific pattern that the pulsed laser beam creates during a process, and this can be seen in Figure 4.

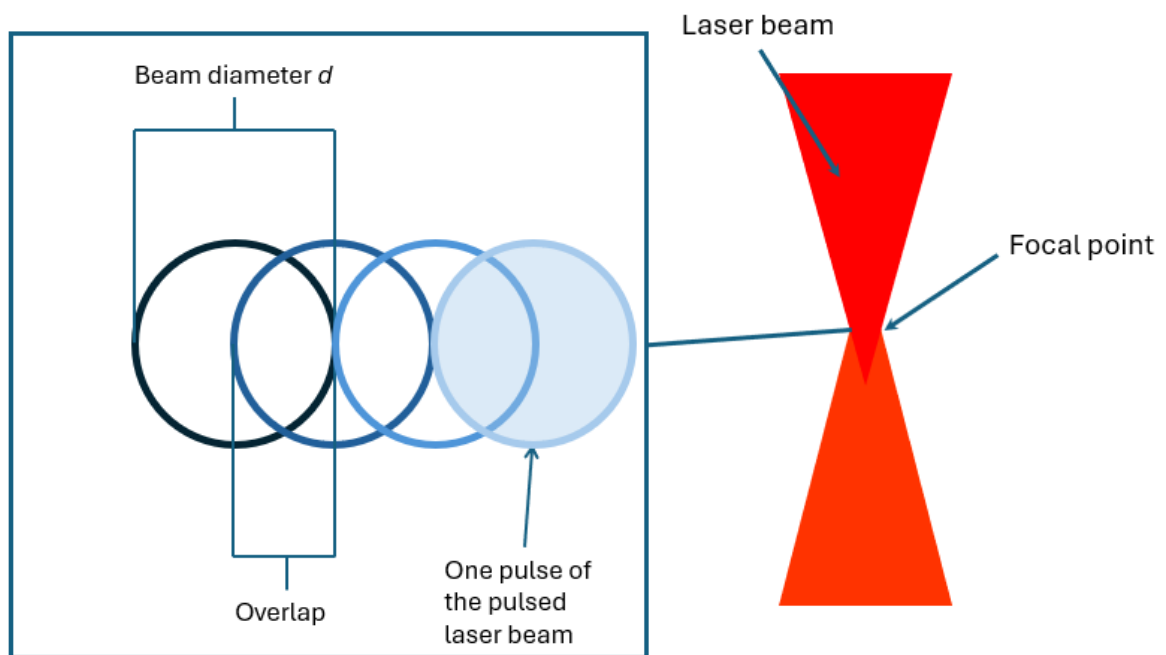


Figure 4. The laser beam (right) and a figure of the pulsed laser beam mechanism (left).

As can be seen from Figure 4, one pulse from the pulsed laser beam creates a circle-shape to the material it was treated with. The surface area of the circle is determined by the beam diameter d . The shape of the pulsed laser beam is an hourglass, as can be seen from Figure 4. A laser beam has a focal point, where the pulse energy is most concentrated, and has the

maximum energy per square meter. This point is where the surface area of the laser beam is the smallest. [23], [24]

As shown in Figure 4 the pulses overlap each other, when a larger area than the area of one pulse is treated. The amount of overlapping of the pulses is determined by parameters, such as the speed of the laser beam motion, pulse period and pulse duration. [24]

A continuous wave laser beam differs to a pulsed laser beam in-terms of continuous excitation energy. When a CW laser beam is compared to a pulsed laser beam, the CW laser beam is a non-interrupted beam, whereas the pulsed beam is in specific intervals with a repetition rate. The CW laser does not have a peak power, the power output is consistent the entire time. [25]

There are different methods of cleaning. One method is by using the different vaporization temperatures as an advantage. When a laser beam is irradiated to a sample, the laser pulse reaches the dirt particle on top of a substrate. The pulse energy creates a vibration in the electron subsystem, because the pulse energy is absorbed by the electrons and converted to heat energy. This heat energy is transferred to the cold material by heat conduction. At the same time the vibrations are transferred to the molecule bonds from the electrons. This leads to the molecule lattice structure to weaken. When the photons from the laser beam have a higher energy than the energy in the bonds between molecules, the bonds break. This means that with enough pulse energy the dirt particles evaporate to a vapour. The mechanism where a material is removed from another solid material by irradiating with a laser is called laser ablation. [6], [26] There is also another method, which takes an advantage of the different vaporization temperatures. This method rapidly heats particles and ejects them off the substrate material. This method is shown on Figure 5.

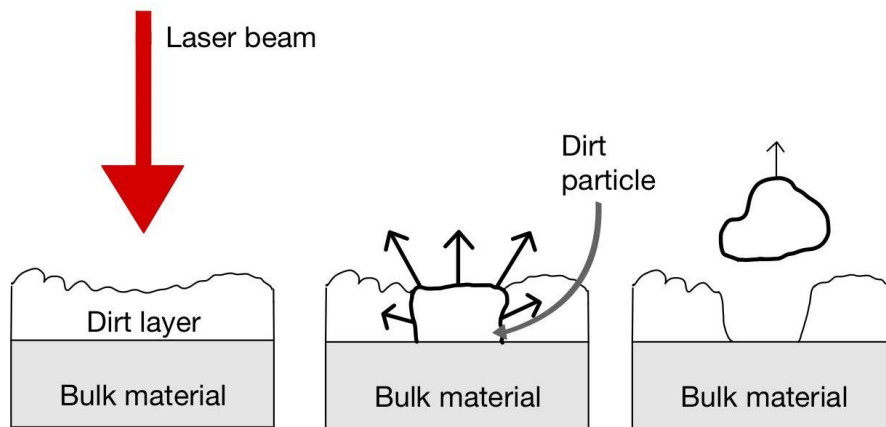


Figure 5. Laser cleaning mechanism. Reproduced from [7] which is under an open access Creative Common CC BY license.

As shown in Figure 5, when a dirt layer and the substrate below it is treated with a laser beam., both begin to heat up because of the pulse energy that is being transferred from the beam to both materials. The rapid heating vaporizes the dirt on top of a substrate but also may eject the particles off from the top of the substrate. [7] , [9] , [27]

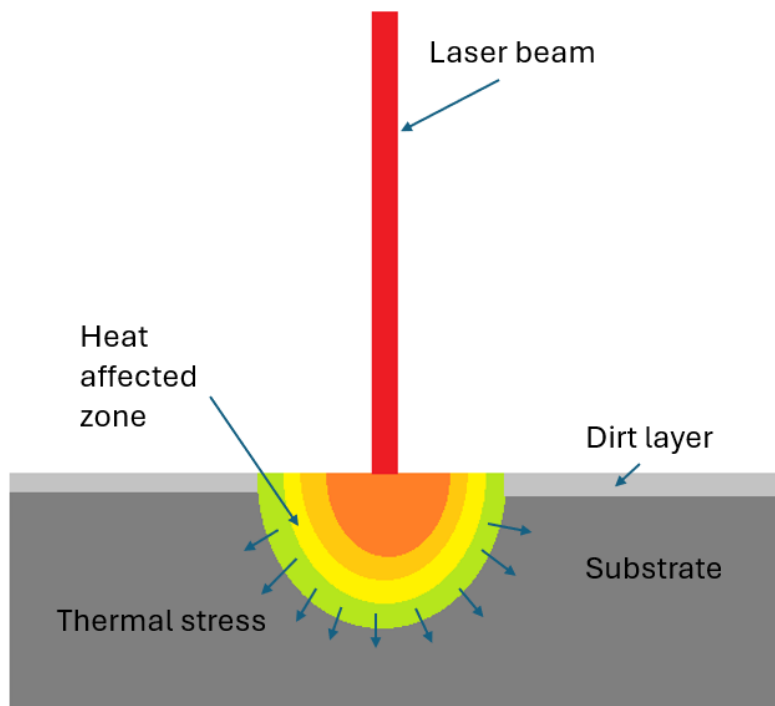


Figure 6. The heat effect of a laser beam to a substrate with dirt layer on top. Reproduced from [27] which is under an open access Creative Common CC BY license.

As shown in Figure 6, the laser beam heats the substrate below the dirt layer. A heat affected zone is the area right next to the laser treated area, that is heated by the laser. This heating causes an inwards expansion of the material, which creates thermal stress in the substrate. In some cases the thermal stresses from the heat affected zone affect the substrate. The incorrect parameters can affect the substrate substantially, and henceforth the end result profusely. [28]

2.2 Research case studies about laser cleaning

Ahn et al. [9] removed oils with older laser equipment. They used a near-infrared laser (Nd:YAG) and a KrF excimer laser from carbon steel, stainless steel and copper. The near-infrared laser has a wavelength of 1064 nm and full width at half maximum of 6 ns. The KrF excimer laser has the full width at half maximum of 25 ns. The oils that were used were a mineral oil and lubricant oil. Before the laser processing, all the samples were smoothed with a sandpaper to have continuous roughness profiles on different materials. The beam was a square, 1mm x 1 mm in size. According to Ahn et al., the Nd:YAG laser was effective on removing

oils from all three materials. The removal of oil began, when the laser fluence was 160 mJ/cm^2 . When the fluence was increased to 210 mJ/cm^2 the oil was removed completely. According to their research, the thickness of the oil coating does not have a significant effect on the oil removal process. In the case of steel, if the fluence exceeded the fluence of 420 mJ/cm^2 , the top surface of the steel started to melt, which means that irreversible damage was starting to form. [9]

Zhou et al. [29] compared two different pulsed lasers to remove oxide film and dirt from the surface of an aluminium alloy to improve the welding quality. The first pulsed laser was a picosecond pulsed laser Edge Wave PX200-1-GM. The pulsed laser has a wavelength of 1064 nm . The pulse width is 10 ps . Another laser used in the article is a nanosecond pulsed laser YLP-V2-1-100-100-100. The wavelength is also 1064 nm and the pulse width is 100 ns . A galvanometer scanning system was used with both lasers. A beam expander was used to have a beam diameter of $38 \mu\text{m}$ in focal point. Argon gas was used in the process as a shielding gas to prevent oxidation. [29]

The inspection for the effectiveness of laser cleaning was done by analysing the depth of the laser path after the cleaning treatment. The best results were achieved with the picosecond pulsed laser, when the laser average power P_{ave} was 100 W , and the overlap was 40% . For the nanosecond pulsed laser, the best results were also achieved with the laser power of 100 W , with an overlap of 60% . According to Zhou et al., the cleaning depth was greater with the nanosecond pulsed laser than the picosecond pulsed laser. When both lasers optimal parameters were compared, the picosecond pulsed laser has better cleaning efficiency. [29]

Cravalho et al. [30] laser cleaned oxidised and Eu-contaminated stainless steel. The laser that they used was an ytterbium fiber laser with an X-Y galvanometric scanner. The wavelength of the gaussian laser beam is 1064 nm and the beam radius is $62 \pm 2 \mu\text{m}$. The maximum average power P_{ave} is 15 W and the pulse duration is 120 ns at full width at half maximum. The repetition rate for the laser pulse was 20 kHz .

According to Cravalho et al. the optimal parameters were that the fluence is 12.4 J/cm^2 with the overlapping of 80% . With higher overlap of 90% the cleaning efficiency improved, but enough energy from the laser was absorbed to modify the substrate surface.

3 Laser polishing

3.1 Overview of laser polishing

Laser polishing is when the laser pulse melts the surface to improve the surface quality. The main idea of laser polishing is to treat the surface of a metal sample with a CW or a pulsed laser pulse with enough average power that the metal reaches its melting temperature. Laser cleaning process very often requires less thermal energy compared to the laser polishing process, as the aim is to melt the material, not to vaporize it. The process of laser polishing is shown in Figure 7.

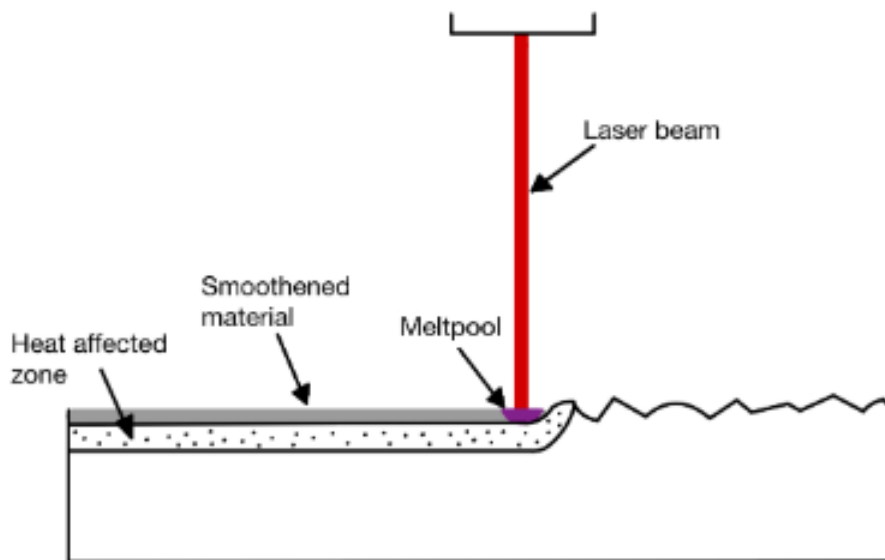


Figure 7. Laser polishing process. Reproduced from [31] which is under an open access Creative Common CC BY license.

As shown in Figure 7, the pulse energy from the laser beam transfers to the electrons and molecules in a similar way with laser cleaning. The pulse energy usually is not as high, so the bonds between the metal crystals, not atoms, are broken and a liquid phase is formed. This creates a melt pool out of the liquid metal. The melt pool has a surface tension, which means that when the metal rapidly solidifies, the surface should be polisher than it was before melting. [3], [32]

If a material has a rougher surface, the peaks are most likely to melt first, because of the heat distribution. the heat does not transfer to the lower material as quickly, and it stays more

localised at the peak, which results in melting. The melting and solidifying is rapid with a pulsed laser because of the periodic high energy density coming from the laser in a single point. [33] The path of the laser beam is shown in Figure 8.

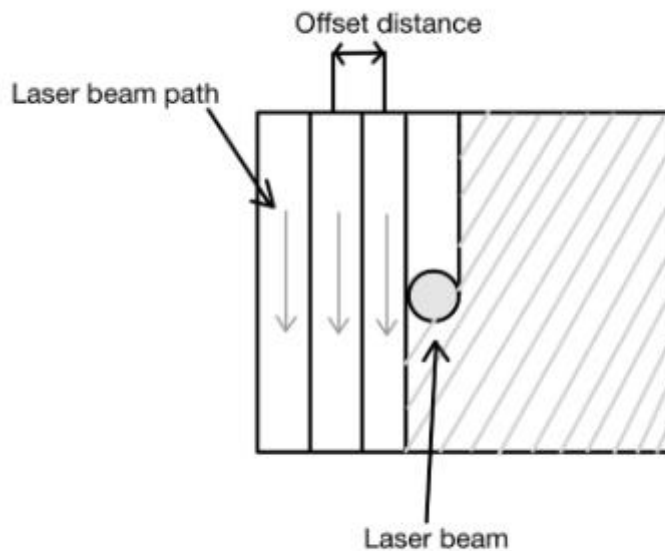


Figure 8. The path of the laser beam in a material. Reproduced from [29] which is under an open access Creative Common CC BY license.

As shown in Figure 8, the offset distance is the distance between two laser beam paths. The offset distance determines, how much overlapping each laser beam path has with each other. If the paths overlap each other, the smoothing is more uniform, since the remelting of some areas connect each melted area to a one smoother surface.

3.2 Research case studies about laser polishing

Sassmanhausen et al. [34] used an ultrashort pulse to smoothen a tool steel (X40CrMnNiMo8-6-4). The laser system used was an ultrashort laser pulse laser FX200-1-GF with a five-axis laser machining system. It has a pulse repetition rate of 48.92 MHz, and pulse duration of 800 fs. Maximum average power P_{ave} is 75W and wavelength of the laser pulse is 1030 nm. During the processing a galvanometer was also used to reach a two-dimensional processing.

The results of the experiments show that the best results were reached, when the single pulse peak laser fluence F_0 was 0.065 J/cm^2 . The significant improvement in the surface roughness was achieved from $0.6 \text{ }\mu\text{m}$ to $0.29 \text{ }\mu\text{m}$ when the scanning speed v of 4.5 m/s was implemented with an overall improvement of 52% . Lowest micro roughness was achieved, when the pulse had an overlap of 0.9973 m/s with a focal diameter of $32 \text{ }\mu\text{m}$. Sassmanhausen et al. mention that the enlarging of the focal diameter, the ripple structures are reduced, and when it is combined with slower scanning speeds, the surface smoothness is improved. According to them an inert gas atmosphere could be used if larger energy inputs are wanted for the polishing. [34]

Temmler et al. [35] investigated how the intensity distribution, fluence and laser beam size affect the area rate and surface roughness of a material. The sample material used was AISI D2, a tool steel. The laser used was a prototype POLAR laser polishing machine, which was set up by Maschinenfabrik Arnold and Fraunhofer ILT. The prototype includes a Yb:YAG disk laser TruMicro 7051 with a maximum power of 550 W and a pulse wavelength of 1030 nm . The repetition rates fluctuated between 5 kHz and 20 kHz . Pulsed mode was used in the experiments, where the pulse durations varied between $1 \text{ }\mu\text{s}$ to $3 \text{ }\mu\text{s}$. The prototype also included a Scanlab laser scanner system that had a VarioScan 30, f-theta objective with a focal length of 420 mm and a HurryScan 25. The laser beam shape was a square, with the side lengths varying between 100 mm , 200 mm and 400 mm . Laser fluence was varied between $4\text{-}12 \text{ J/cm}^2$ in all three beam sizes. The pulse energy was different between all beam sizes. The 100 mm beam side size laser power varied between $8\text{-}24 \text{ W}$, the 200 mm was varied between $32\text{-}96 \text{ W}$ and lastly the 400 mm beam size laser power was varied between $128\text{-}384 \text{ W}$. Argon gas was used as a shielding gas. [35]

The analysis was done with a stereo microscope M205 C from Leica Microsystems. Temmler et al. mention that since the stylus roughness measurement is not as effective, a systematic white light interferometry (WLI) measurement was done to measure the S_a values from the laser polished surface. This measurement was done with Newview 7300 from Ametek-Zygo with the software Zygo MetroPro (V10.3). [35]

Temmler et al. conclude that increasing the laser beam allows the usage of higher pulse energies and larger average power. With the fluence of 4 J/cm^2 the material did not melt and if the fluence was 12 J/cm^2 , the material evaporated. The lowest surface roughness was achieved with a laser pulse length side of 400 and fluence of 8 J/cm^2 . [35]

4 Overview of corrosion

Corrosion is an important aspect of maritime industry in the context of safety, conservation and economics. The aim to study corrosion is to reduce the material losses in ships, bridges and other structures that are exposed to corrosive environment. All metal that is lost for corrosion does not just mean material losses. There are also other resources that are needed, such as water and energy. Most substantial are the economic losses. [20], [36]

Corrosion is a chemical reaction of a metal in a corrosive environment which causes the metal to deteriorate and produce oxides. The electrochemical explanation is that a corrosive environment, such as saline solution and a metal create a short-circuited galvanic cells. The metal loses electrons to the saline solution, which creates metal ions called as anodic reaction, or oxidation. In case of a saline solution or for example the atmosphere, the electrons from the metal react with water and oxygen molecules, which creates hydroxide ions called as cathodic reaction, or reduction. In the end the metal ions and hydroxide ions react and in the case of for example iron, create rust (iron oxides) on top of the metal. [16], [20]

A structural steel in marine environment, which includes immersion, coastal atmosphere and splashing, usually corrodes in a uniform manner, if the steel is unprotected. This means that the corrosion is approximately the same in all exposed area with the same conditions. The corrosion causes a loss of thickness of the steel, where for example a load bearing steel structure may fail. A layer of rust forms to the corroded areas, and marine organisms and sediment can form to the rusty areas. Under the layer of rust another common forms of corrosion may form and create localised corrosion as pitting or cracks. The localised corrosion is particularly dangerous, as it may be difficult to detect. [15], [20]

Overall stainless steels corrode less compared to regular steels. This does not mean that stainless steel does not corrode at all. In fact, the corrosive sea water in marine environment influences the cathodic reaction between stainless steel and sea water. [14]

The environment of the metal affects greatly on what the composition of the corrosive solution is when corrosion is simulated. The corrosion tests are specially designed and standardised to produce as accurate results as possible. A neutral salt solution can be used in experiments as an electrolyte to simulate a general sea environment,. [14] [37]

One of the ways corrosion can be measured is by using three electrodes, working electrode, reference electrode and counter electrode in a corrosive solution. The reference electrode monitors the potential of the system, and the counter electrode maintains the current flow in the corrosive environment. Working electrode includes the sample of which the corrosion values are measured. The circuit is connected to a computer with a software suitable for electrochemical measurements. The potential of the circuit can be changed from the software. a tafel plot. [38] An example of this can be seen in Figure 9.

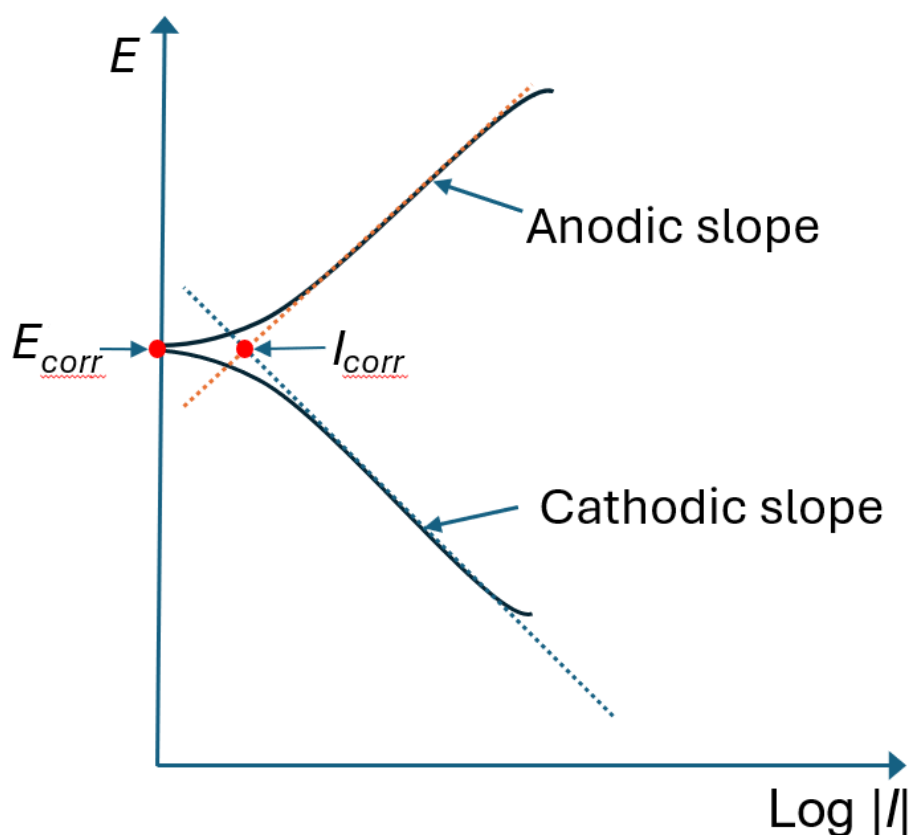


Figure 9. Tafel plot with anodic and cathodic slopes with E_{corr} and I_{corr} values. The I_{corr} values are in logarithmic scale.

As shown in Figure 9, a tafel plot is an E-I curve, where the I is in logarithmic scale. The tafel plot consists of two separate slopes, anodic slope and cathodic slope. The anodic slope represents the oxidation phase and the cathodic slope the reduction phase. When tangents are drawn according to the slopes, the intersection of the tangents represents I_{corr} , called as the corrosion current density. The unit of I_{corr} is amperes per cm^2 , or A/cm^2 . A high I_{corr} value

suggests that the sample corrodes faster, a lower value means slower corrosion. From the intersection another value can be obtained, E_{corr} which means the open circuit potential. The units of E_{corr} is volts, or V. A higher E_{corr} value indicates that the sample is more stable and passive. A lower E_{corr} value does not always indicate that the corrosion as a process is faster. [38], [39]

Corrosion rate is another important factor, when considering the corrosive effects and development in a material usually derived from uniform corrosion loss and the amount of time exposure. It can be concluded that the corrosion rate is the average metal thickness that is lost in a year, the unit is mm/y. Corrosion rate helps to understand the service life of a metal in a specific environment. [15], [38]

Specific constants from the material are required, when corrosion is calculated. Since the atomic composition is different, they work differently in corrosive environments. Important constants are density of the material, surface area of the area which is corroding and equivalent weight.

The equivalent weight, EW , is the amount of metal in grams that is oxidised, the amount of one Faraday of electric charge passes through the material. There is an equation for alloys, which is

$$EW = \frac{1}{\sum \frac{n_i * f_i}{W_i}} \quad (2)$$

Equation (2) includes n_i , which is the valence of the i^{th} element in the alloy, f_i which is the mass fraction of the i^{th} element in the alloy and W_i which is the atomic weight of the i^{th} element in the alloy. [40]

5 Aim and purpose of experimental part

The aim for the study is to assess the effects of laser pre-and post-treatment on the marine-grade steel (EH36). The goal is to study the effects of the laser processing with microscopy and inspect the corrosion resistance while comparing all different stages of laser processing to each other. The experimental part in this thesis can be divided into three parts. Figure 10. describes the three different stages and shortly describes what experiments each stage includes.

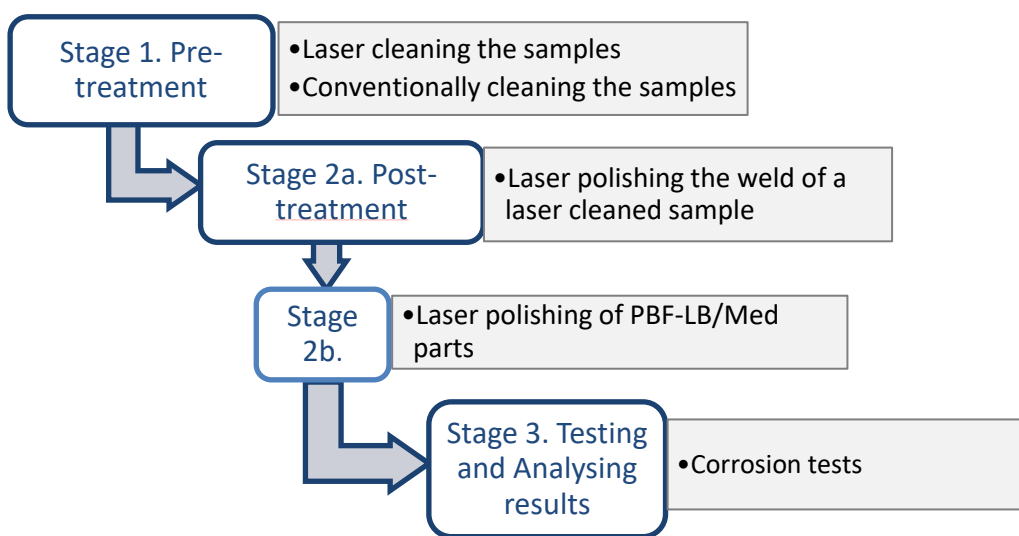


Figure 10. Stages of study for this thesis.

As shown in Figure 10, the first stage is pre-treatment of the steel plate that has been soiled, rusted and greasy is laser cleaned and conventionally cleaned. Preliminary testing was done before the laser cleaning to determine the optimized parameters. After the preliminary testing the laser cleaning was done with the chosen parameters. Lastly the 2 plates with the same cleaning method are welded together.

The second stage is post-treatment. In part 2a. after the welding has been done, the weld is smoothed. A series of preliminary testing was also done for the laser polishing. The laser polishing is done only for the laser cleaned sample. Part 2b. is the laser polishing for additively manufactured sample. Preliminary testing was also conducted to achieve good results. As the

laser polishing is performed on the laser cleaned samples only, the discussion in part 2 is between laser cleaning and laser polishing.

The last stage is testing the samples and analysing the results. All different samples are inspected first with a microscope, then optical microscope Bruker Alicona and lastly corrosion tests are performed. After the different tests, the analysis is completed for the test results.

The scope of the study was limited to laser cleaning as a pre-treatment, laser polishing as a post-treatment and how those affect the corrosion resistance of the metal, since any additional testing such as tensile testing or hardness testing would increase the amount of data for the thesis significantly. These would also increase the experimental time. Because one of the important aspects in this thesis is maritime industry, the focus was set on microscope imagery and corrosion testing.

6 Experimental setup

6.1 Maritime industry EH36 steel

The material that is used in the experimental work is NV E36 (EH36), a low alloy (HSLA) steel produced by SSAB. This steel grade is mainly used in ship building industry, and this why it was chosen for experiments for this thesis. EH36 has good toughness values, great welding properties and has high strength. This steel also has good corrosion resistance, which is important for a steel that is in the marine environment. [41], [42]

The steel was produced by hot rolling, with a thickness of 4 mm and class grade B. The chemical compound and mass percentages of the steel can be found in Table 1. The material has a density of 8.16 g/cm³.

Table 1. Chemical composition-% of NV E36 steel plate.

Elements													
C	Si	Mn	P	S	Al	Nb	V	Ti	Cu	Cr	Ni	Mo	Ca
0.055	0.2	1.35	0.009	0.002	0.03	0.025	0.008	0.016	0.012	0.05	0.04	0.005	0.002

As can be seen from the Table 1, the three main elements in the steel besides iron are carbon, manganese and silicon, with iron being in balance. The steel complies with the European Standard EN 10029:2010, which is the standard for hot-rolled steel plates that are 3 mm thick or above and includes tolerances on dimensions and shape [43]. More of the material properties can be found on Table 2, where the results from the manufacturer about the tensile test made for the steel are listed.

Table 2. Material values from tensile test done by the manufacturer of the steel.

Tensile test			
K2	Upper yield strength (MPa)	Ultimate tensile strength (MPa)	A %
31	481	537	30

As shown in Table 2, because the material has the upper yield strength of 481 MPa and relatively good ductility of 30 %, the steel is suitable for applications where it needs to withstand high strengths without deforming or having brittle behaviour. This is why it suits the maritime applications. The ultimate tensile strength of 537 MPa tells that the material has high strength. When compared to the upper yield strength, the ultimate tensile strength is higher than

the upper yield strength. This means that as the material starts to deform, it hardens. The stress deformity factor K2 with the value of 31 means that the material has high deformation resistance. When all is combined with the elongation of 30 %, the material has good ductility, and it can deform a lot before breaking.

6.2 PBF-LB/M of 316L stainless steel

Another material used in the experiments is a 316L stainless steel. The stainless steel has been produced with additive manufacturing (PBF-LB/M) out of powder with EOS M 290 machine. The stainless steel is a marine grade, high performance austenitic stainless steel. The main characteristics include high strength, ductility and toughness. The EOS stainless steel also has high corrosion resistance, which means that it would be suitable for maritime industry. [44]

Table 3. Chemical composition of the EOS StainlessSteel 316L [44]

Element	Fe	Cr	Ni	Mo	C	N
Min	Balance	17.0	13.0	2.25	-	-
Max		19.0	15.0	3.00	0.03	0.10

As shown in Table 3, besides iron, the material that the alloy consists most of is chromium with 17-19 wt.-%. The material corresponds to ASTM F138 standard. The standard is a material standard for surgical implants, also UNS S31673. The powder has a generic particle size distribution, which is between 20 μm and 65 μm . The material may also be heat treated with stress relieve (temperature 900 °C, hold time 2 h) or solution annealing (1150 °C, hold time 1.5 h). [44] The plate sizes are shown in

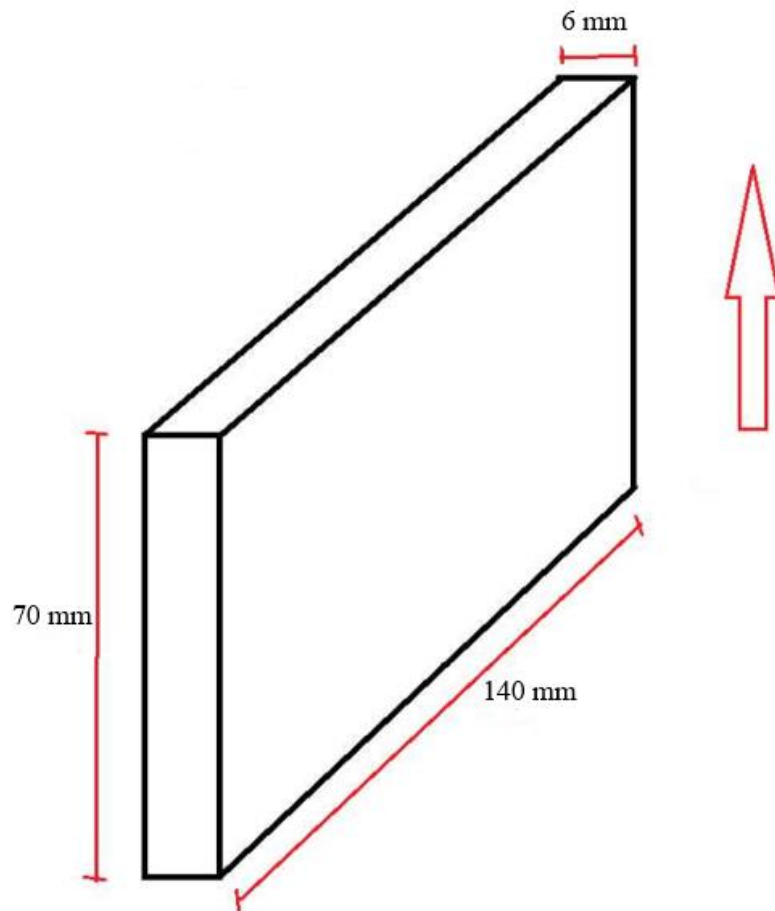


Figure 11. The building dimensions and printing direction of the sample.

As shown in Figure 11, the dimensions of the plate were 140 mm x 70 mm x 6 mm. The red arrow indicates the build direction of the sample plate. This means that the sample was attached to the build plate on one of the sides with the dimensions of 140 mm x 6 mm.

6.3 Hardware

Nanosecond pulsed fiber laser

The machine that is used in the laser cleaning and laser polishing is a IPG YLPN nanosecond pulsed fiber laser and scanner. The laser has a built-in scanner head with the operating area of 100 x 100 mm. The wavelength has a minimum of 1055 nm and a maximum of 1075 nm. Typically it is 1064 nm. The maximum average power is 100 W. The focal point is at 283 mm from the lens of the laser and the beam diameter is ~60 μm . The work area has a metal cover on three sides for protection of the user.

The laser is in a normal indoor air environment, which means that air enters the work area. The air combined with the heat from the laser pulse may cause the sample to oxidize, which is why argon was used in the set up as a protective gas. The argon flow was 25 ml/s. Figure 12 shows the setup for the laser equipment.

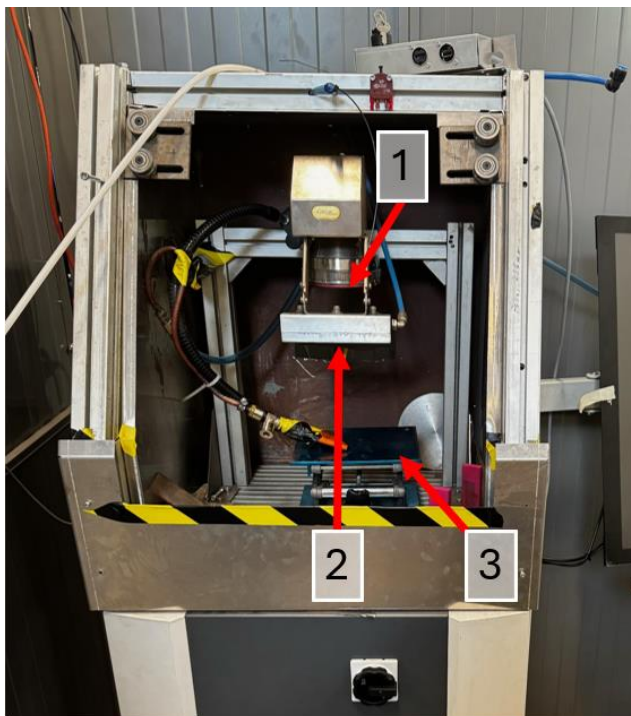


Figure 12. Pulsed laser setup for laser cleaning and laser polishing.

As shown in Figure 12, the laser setup includes the laser (1), an air nozzle (2) which blows regular room air almost horizontally to prevent fumes or sparks from laser processing to reach the lens of the laser and causing damage. There is also the working area (3), that can be raised

or lowered depending on the thickness of the sample. A closeup of the setup is shown in Figure 13.

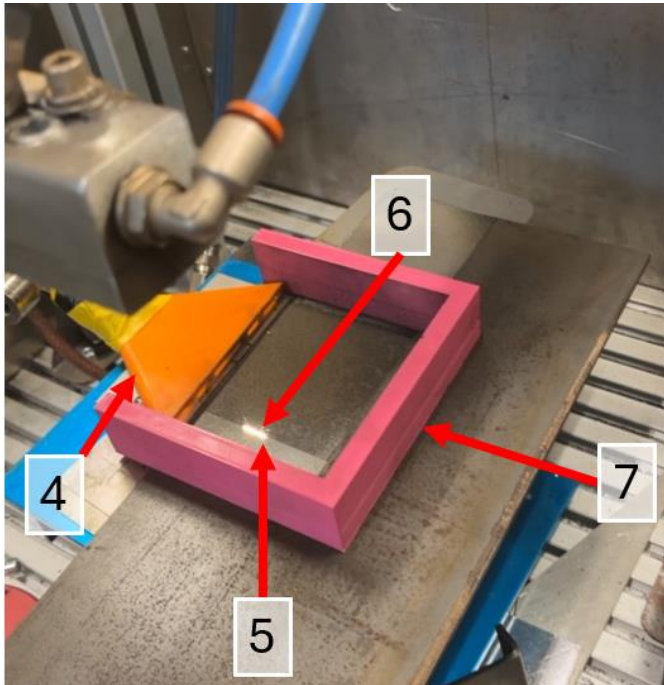


Figure 13. Closeup of the laser setup.

As shown in Figure 13, the figure shows a real time image of the laser cleaning process. The laser process can cause oxidation in the sample, which is prevented with argon gas. The setup has a wide argon nozzle (4) so that the argon reaches the whole treatment area. As the sample is being cleaned, the cleaned side can be seen as a lighter area (5) compared to the rest of the sample. The laser beam (6) is moving quickly which is why it appears to be wider, but in reality, the beam diameter is $\sim 60 \mu\text{m}$. Lastly, there is a barrier (7) to keep the argon gas in the surface as long as possible.

EOS M 290

EOS M 290 is a medium-sized AM system that utilises metal powder to produce metal parts based on a 3D model, for example a CAD design. It uses a 400 W Yb-fiber laser to melt the powder in the desired points to manufacture the product. The system has a high-speed scanner with the maximum scan speed of 7.0 m/s. The build volume of the system is 250 x 250 x 325 mm. The materials that can be used with the system range from multiple aluminium alloys and stainless steels to nickel alloys and multiple titanium grades. The system uses a protective gas, such as argon. [45]



Figure 14. EOS M 290 additive manufacturing system. [45]

Corrosion measurement setup

The corrosion measurement was made by using a Gamry instruments surface corrosion system with Ivium electrochemical analyser. Figure 15 shows the setup for the measurement.

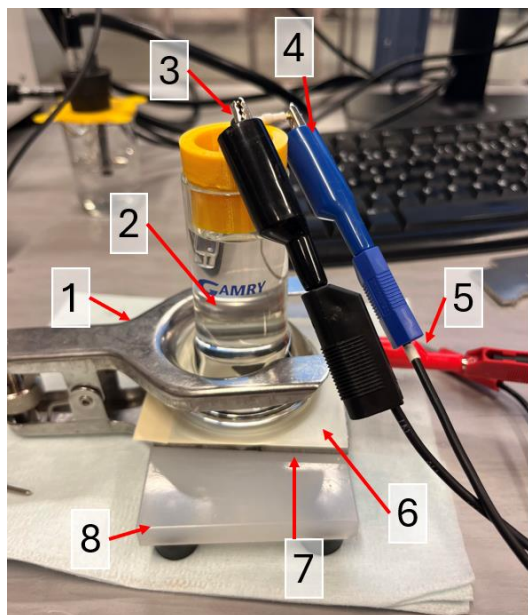


Figure 15. Corrosion setup.

As can be seen from Figure 15, a clamp (1) holds the beaker with a saline solution (2) tightly against the sample. Electrode and reference electrode together with the clamp in the sample create an electric circuit. The current goes through the sample and the saline solution to the Ivium electrochemical analyser. The mask (6) on top of the metal sample (7). The mask allows the analysed area to be smaller, a circle with a radius of 1 cm with area of 0.785 cm^2 . The whole setup is on top of a plastic stand (8).

Bruker Alicona Infinite Focus G6

Bruker Alicona Infinite Focus G6 is an optical measurement system. The main applications for the system are surface measurements and profiles. It uses laser imaging with a coordinate system to create a 3D dot cloud images. The images capture both the topology and the geometry of the surface. The resolution is up to some nanometres, with a magnification starting from 5x all the way up to 100x. This measurement system can take images of all sorts of materials and surfaces to create the images. The measurement system uses a MetMax 3.0 software to analyse the images taken with Alicona.

In this thesis, the Alicona system was used to measure the R and S roughness values. It was also used to take images that show the height difference in each part of the taken image. Geometry of the welds was studied with the values retrieved from the Alicona images. Figure 16 shows the Alicona system.

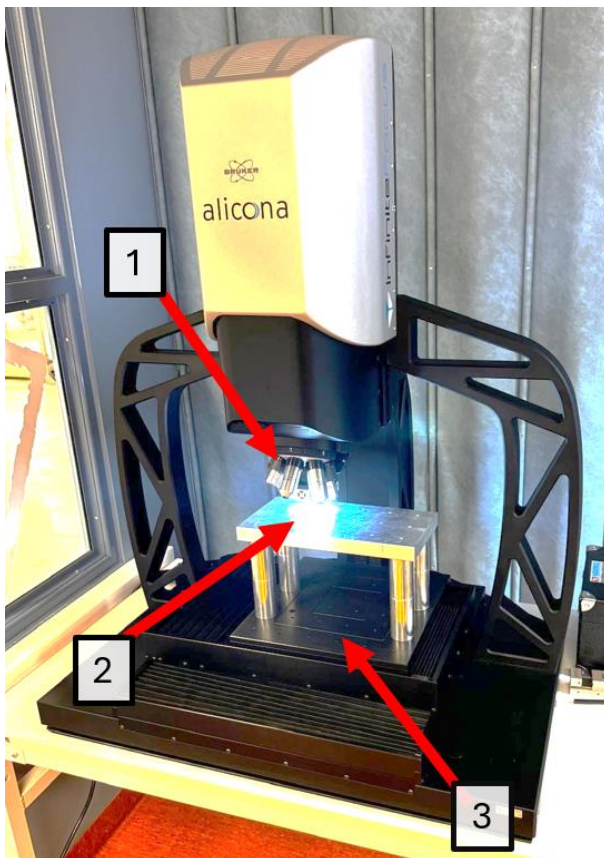


Figure 16. Bruker Alicona Infinite Focus measurement system.

As shown in Figure 16, the lenses (1) are chosen based on what magnification is required. The sample is placed on the sample holder (2). The system has also a moving platform (3) to make sure that the lenses stay stable.

7 Experimental procedure

7.1 Material preparation

The samples need to mimic the conditions of maritime warehouse to test the effectiveness of laser cleaning and laser polishing. The samples are treated with an oil to prevent the surface from rusting in a maritime warehouse. During the machining some cutting fluid could also spray on to the surface. With an oily surface, the material would be stored before any surface preparation and used in a ship.

The material was laser cut into plates of 400 x 150 mm for easier handling. The plates would be much larger in real-life conditions. The sample preparation was started by creating some rust to the surface of the samples. Firstly, the plates were rusted using a saline solution mimicking real-life marine conditions in the Baltic Sea. The samples were kept in the solution for 48 hours to achieve a realistic rusting and corrosion on the surface. Secondly, the plates were kept in the saline solution, the samples were left to dry for 72 hours. This would ensure that the plates are rusted well, since airdrying leaves the plates well in contact with oxygen.

After rusting, some of the dried salt flakes were scrubbed off. Then the samples were sprayed with a rust preventive oil and cutting fluid. The amount of oil and fluid were $\frac{3}{4}$ of oil and $\frac{1}{4}$ of fluid.

7.2 Pre-treatment (Part 1)

The main goal in laser cleaning is to remove all the dirt and oil on top of the plate. Because of time and equipment restrictions, these parameters were chosen based on literature and visual inspection in this thesis. During the laser processing argon as a protective gas was used with the flow rate of 25 l/min.

The preliminary testing for the laser cleaning was conducted with a matrix of eight squares. One square had the area of 1 cm². The matrix was formed with two squares in a column, and four squares in a row. The testing was done with such small areas to quickly determine the correct parameters. The parameters for the preliminary testing can be found from Table 3, additional information is on the Appendices Table 9. Focal point was set to the surface of the material.

Table 4. Preliminary testing for laser cleaning.

	Speed (mm/s)	Laser power (W)	Fluence (J/mm ²)
1	450	25	17.68
2	450	50	35.37
3	450	75	53.05
4	450	100	70.74

As shown in Table 4, the speed was kept constant of 450 mm/s. The power was varied between 25 W – 100 W. Fluence was calculated with equation (1). The choice for best parameters was made with a visual inspection, when the plate seemed to have all the dirt removed. The parameters that were used in the laser cleaning of the plates can be found from Table 5.

Table 5. The best parameters for laser cleaning.

	Speed (mm/s)	Laser power (W)	Pulse frequency (Hz)	Pulse width (µm)	Treatment rounds
Chosen parameters	450	25	100 000	0.075	4

As shown in Table 5, the best parameters were with power of 25 W, pulse width of 0.075 µm. Because the one treatment round was not enough to clean the surface, the best result was with four treatment rounds per area. Figure 17 shows how the area of the sample was laser cleaned.

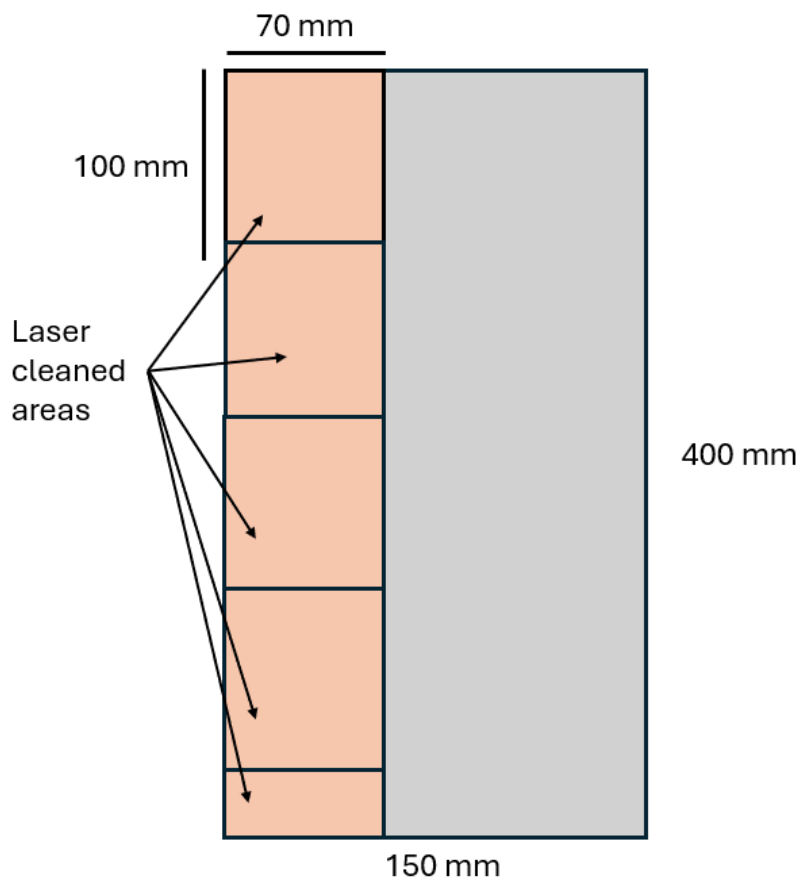


Figure 17. The laser processing area for laser cleaning.

Since the area for laser processing is quite small, only 100 x 100 mm, the entire sample could not be cleaned with one treatment round. Henceforth, the sample was cleaned in four segments, with each having the area of 70 x 100 mm, as shown in Figure 17. Areas were slightly overlapped of 4 mm, to ensure that there were no areas left untreated. The small area is the result of overlapping was left at the end of every plate, which was also cleaned with a laser. The treatment area of the width of 70 mm was chosen to make sure that the oil does not seep immediately to the weld area, since the entire plate was not cleaned to save time. The sides of the plates were also cleaned with laser using the same parameters as to the rest of the plate. This step is important, since it affects most the weld and any impurities can cause defects to the weld.

After cleaning was done, the samples were welded with a CW laser. As the welding is not focused of this thesis, it is not specified further. The welding parameters can be found from the appendices in Table 12.

Conventionally cleaned samples

The conventionally cleaned samples were cleaned with a cylindrical grinding setup. The setup has a rotary axis with aluminium oxide grinding paper. The rotation speed of the set up was set to 180 rpm. With the sample height of 400 mm and width of 4 mm, it took 4 – 5 minutes to reach satisfactory cleaning results.

7.3 Post-treatment (Part 2a)

After welding, the nanosecond pulsed laser was used to smoothen the weld as well. The parameters were determined in a similar way as the cleaning was done. The same set of parameters were used for laser polishing. The parameters that made the most melted surface were chosen, as the melting creates the smooth surface in laser polishing. A more detailed information on the parameters can be found in the Appendices Table 9. Some inspection was also done with Alicona measurement system to visualize the melted surface better with profile figures. Table 6. shows the parameters for the post-treatment laser processing.

Table 6. Chosen parameters for laser polishing.

	Speed (mm/s)	Laser power (W)	Pulse frequency (Hz)	Pulse width (μm)	Treatment rounds
Chosen parameters	450	75	100 000	0.025	6

As Table 6. shows, the speed of 450 and pulse frequency of 100 000 Hz were the same as in laser cleaning. The laser power was set to higher compared to the laser cleaning process with the laser power of 75 W. Pulse width was shorter in the laser polished parameters as the value is 0.025 μm . The treatment rounds were set to six to achieve a smooth molten surface. Since the polishing affects the weld the most, an area of 1 cm x 10 cm was chosen for the smoothing of the weld.

7.4 Post-treatment of PBF-LB/M (Part 2b)

The additively manufactured part was built at EOS by using EOS M290 system. The finished part had the dimensions of 140 mm x 7 mm x 6 mm. The layer thickness of the part was set to 40 μm .

The same matrix procedure for laser polishing was done for the additively manufactured part as was with the welded part. The preliminary parameters were also the same. The final parameters used for the polishing were different compared to the welded sample. They can be seen in Table 7.

Table 7. Parameters for laser polishing PBF-LB/M sample.

	Speed (mm/s)	Laser power (W)	Pulse frequency (Hz)	Pulse width (μm)	Treatment rounds
Chosen parameters	450	75	100 000	0.075	6

As shown in Table 7, the parameters are similar to the part 2a parameters. The pulse width has been set wider compared to part 2a. Longer pulse width is more suitable for melting the material as the pulse energy is spread to a wider area. This means that the area one pulse treats is not heated as much that it vaporizes, which is the case in laser cleaning. The area melts as it should during a laser polishing process. The material choice (316L) also effects on how it performs during the laser polishing process. The melting point is different compared to the EH36, which means that slight variation in process parameters might be required. All other parameters are the same as in part 2a.

7.5 Testing and analysis (Part 3)

All of the samples are characterized with an optical measurement system Bruker Alicona G6 after the laser processing. The images taken were 5 mm x 3.6 mm. The lens with a magnification of 20x was used for obtaining images of the samples.

Since the images are actually 3D surfaces created out of thousands of datapoints, the images can be analysed and values such as roughness values can be obtained. Before analysing all the images a reference plane was set for all images. This was done by the software in the Alicona system MetMax 3.0, where all of the datapoints are taken into account and the program calculates the average height point based on them.

The roughness values Ra, Sa, Rz and Sz were measured with Alicona system. The measurements were performed three times to obtain an average value.

The corrosion test measurement required the Gamry instruments surface corrosion system with Ivium electrochemical analyser. Since the context of this study is in maritime industry, the metal sheets should be tested in an environment which represents the maritime industry to mimic artificial sea water. The water was prepared according to ASTM D 1141-98 standard to the pH value of 8.20 adjusted with 0.1 M of NaOH solution. [46]

The data acquired from the corrosion test setup is a tafel plot. The area of the corroded sample, equivalent weight and density should be known for the accurate results. The calculated values are shown in Table 8.

Table 8. Equivalent weight, surface area and density of both sample materials.

	Equivalent weight (g)	Surface area (cm ²)	Density (g/cm ²)
Steel	10.8	0.785	8.16
PBF-LB/M of stainless steel	11.7	0.785	8.00

As shown in Table 8, the values are similar to each other, but some small changes can affect the end results from the tafel plots. Equivalent weight is slightly more in the stainless steel than steel. Density is slightly higher in steel compared to the stainless steel. The equivalent weight was calculated based on the elements listed on Table 1 using the equation (2) for equivalent weight. The weight and the size of the sample were measured to calculate the density of the sample. Surface area was calculated with the knowledge of the corroding area circle radius of 10 mm.

8 Results and discussion

This section shows the results and discussion chronologically in three parts. First part (Part 1. pre-treatment) focuses on the laser cleaning results and comparison to the conventional methods. The second part (post treatment (part 2)) is centred around the laser polishing and its comparison to the Part 1. results. The last part (Part 3. Analysis) focuses on the corrosion results and how all different methods compare to each other. Figure 18 shows all of the eight samples that are further inspected and analysed.

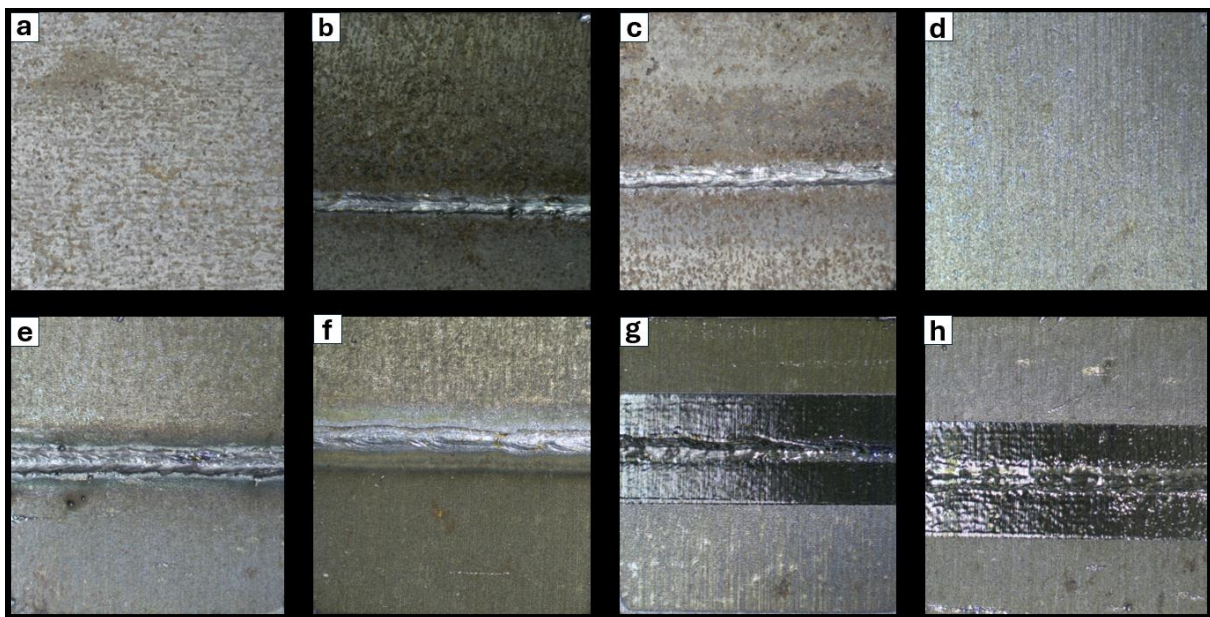


Figure 18. All eight different samples made of EH36 that are analysed.

As shown in Figure 18 there were eight samples made of the EH36 steel. Samples a-f are part of Part 1 and g-h are part of Part 2. The first sample a is a non-laser treated sample with dirt on top, samples (b-c) are cleaned with conventional methods before welding, d-f only have laser cleaning method used. Lastly g-h have been laser cleaned and also laser polished.

8.1 Pre-treatment (Part 1)

There were two different pre-treatments, conventionally cleaned (shown Figure 19) and laser cleaned (shown in Figure 20). Both figures have the weld horizontally. The scale is indicated by the red line, which is 5 mm in length.



Figure 19. Welded sample with conventionally cleaned side as a pre-treatment.

As shown in Figure 19, the weld can be seen in the middle with horizontal orientation. The scale is 5 mm, and this is indicated by the red line in the bottom right corner of the figure. The weld is not smooth and the dirt and rust is visible. The dirt particles, oil and rust appear as the brown specs all over the sample. The laser cleaned sample can be seen in Figure 20.

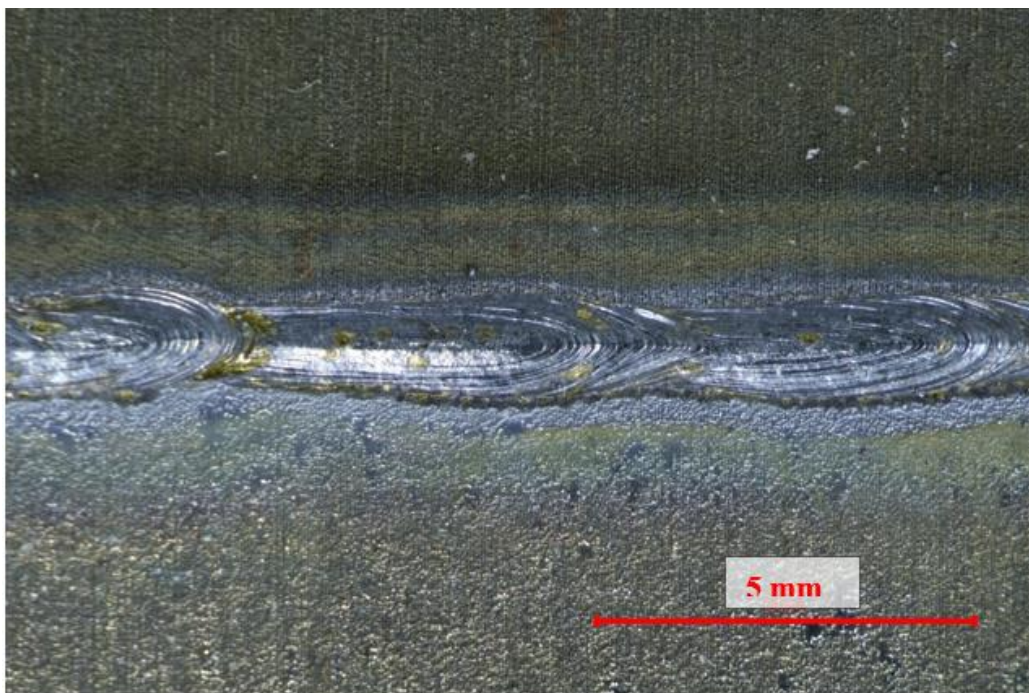


Figure 20. Welded sample with laser cleaning as a pre-treatment.

As shown in Figure 20, the weld can be seen in the middle with horizontal orientation. The scale is 5 mm, and this is indicated by the red line in the bottom right corner of the figure. Some colour differences can be seen next to the weld, which may have been caused by the heat from the welding process. This can be seen much more clearly in the laser cleaned sample than the conventionally cleaned sample in Figure 19.

Both Figure 19 and Figure 20 are from the bottom of the weld. Figure 20 clearly shows, that the area next to the weld does not have the same rust particles as are visible in Figure 19. From this can be concluded that some dirt has been able to remove from the plain surface. However, the effects on the weld cannot be determined from these figures only. The bottom profiles of the welds can be seen more clearly in Figure 21. The figure shows the profile of the profiles as length in mm as the function of height in μm .

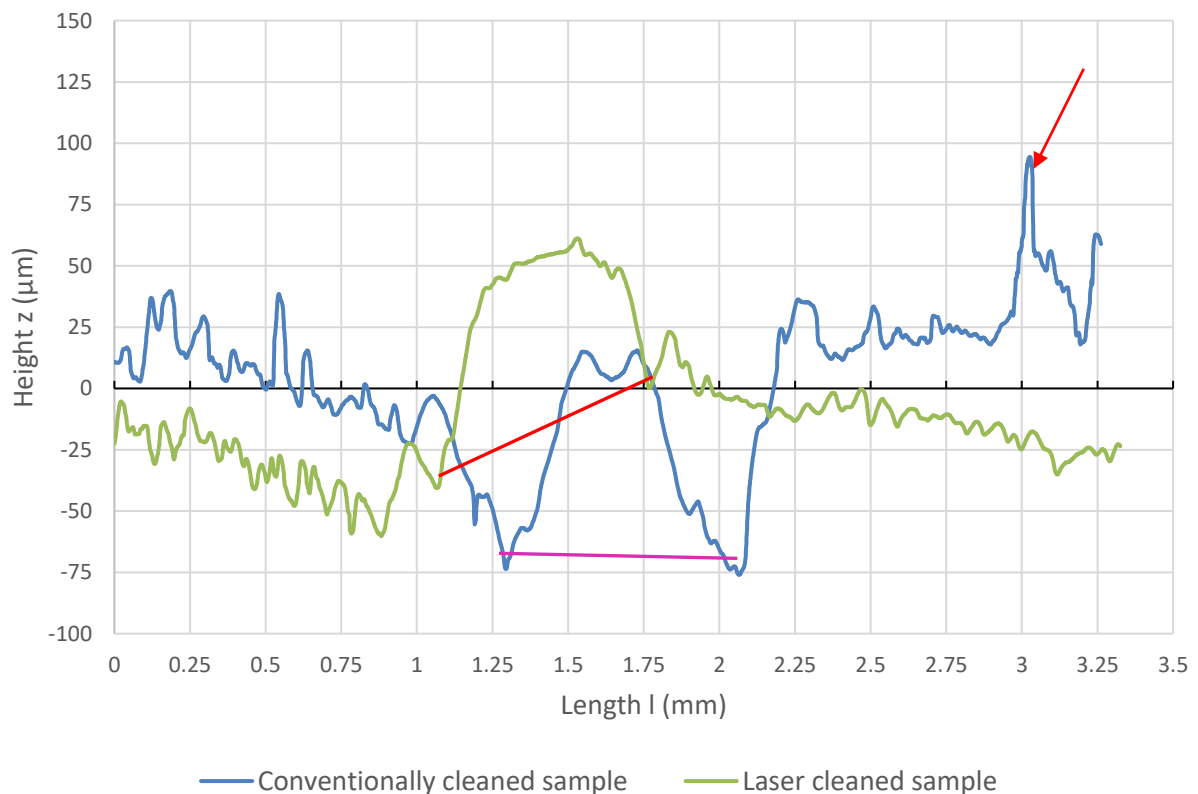


Figure 21. Profiles from the weld from conventionally cleaned (blue) and laser cleaned (green) samples. Red line shows the place of the weld for the laser cleaned and purple shows the place of the weld in conventionally cleaned sample.

As can be seen from Figure 21, the blue profile is the conventionally cleaned bottom and the green profile is the laser cleaned bottom of the sample. The zero point on the y-axis is the

reference plane set by the software based on all of the datapoints. The lines indicate the place of the welds, red for the laser cleaned weld and purple for the conventional weld.

At first both of the profiles decrease. Conventionally cleaned decreases further, almost to 80 μm , when the laser cleaned decreases to 60 μm . The weld starts at around 1 mm in both of the profiles. The laser cleaned sample weld profile is increasing until it reaches the apex at around 1.5 mm and the height of 60 μm . After that the laser cleaned weld profile decreases steeply to around 1.75 mm and then profile decreases slightly. The conventional weld first from 1 mm – 1.25 mm length decreases and then increases from 1.25 mm – 1.5 mm. The peak of the weld is at 1.6 mm, but there is a small increase at the peak, with the height of 15 μm . After the peak the conventionally cleaned profile again decreases from 1.75 mm – 2.0 mm and increases from 2.0 mm – 2.25 mm until it only slightly increases.

There is more of overall roughness in the conventionally cleaned profile, since there are higher peaks around the weld when compared to the laser cleaned profile, for example one is located at the length of 3 mm in the conventionally cleaned profile. One of the reasons for the difference in the roughness is that the laser cleaned samples were cleaned from the vertical and horizontal sides, when the conventional were only cleaned vertically. This means that there is some rust on the sides of the conventional weld that creates the higher peaks, which is indicated with the red arrow in the Figure 21. Differences in weld profiles overall are quite large, as the conventional weld has sinking next to it while the laser cleaned does not. This can be a result of the laser cleaning process. It can also be just a welding defect caused by the welding process itself. A more similar shape can be seen in Figure 22, where the profiles of the top of the welds are inspected.

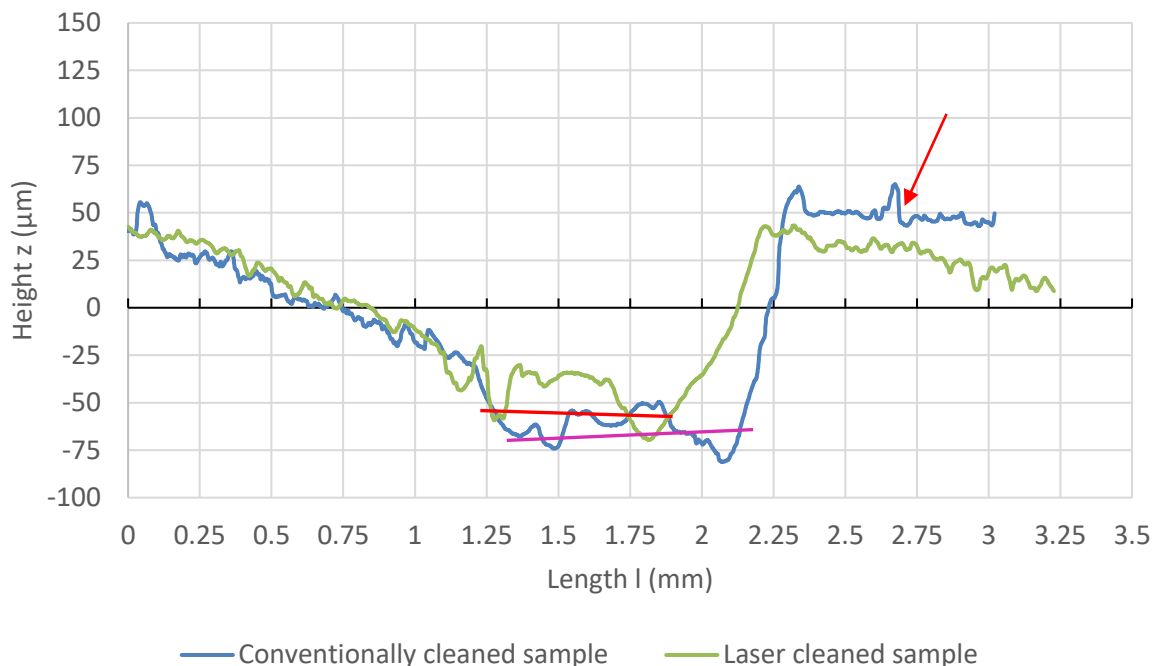


Figure 22. Profiles from the weld from conventionally cleaned (blue) and laser cleaned (green) samples. Red line shows the place of the weld for the laser cleaned and purple shows the place of the weld in conventionally cleaned sample.

As shown in Figure 22, similarly to Figure 21 the blue profile is conventionally cleaned sample and the green profile is the laser cleaned sample. The red line indicates laser cleaned sample's weld and purple line conventionally cleaned samples weld. Both of the profiles decrease in a similar angle from the beginning (0 mm), until they reach the lowest point of the profile, laser cleaned profile at the length of 1.8 mm and height of $-70\ \mu\text{m}$ and the conventional at 2.1 mm and $-80\ \mu\text{m}$. These minimum values also include both welds, laser cleaned weld is in between 1.25 mm – 1.8 mm and the conventionally cleaned weld is between 1.5 mm – 2.1 mm. After the weld and minimum points, both profiles steeply increase. When the laser cleaned profile reaches the height of $40\ \mu\text{m}$ at the length of 2.2 mm, it slightly decreases from 2.2 mm – 3.0 mm. The conventionally cleaned profile increases until it reaches the height of $60\ \mu\text{m}$ at 2.3 mm and then almost stays level between 2.1 mm – 3.0 mm.

The conventionally cleaned profile has higher roughness peaks when compared to the laser cleaned profile, which was stated in the bottom profiles as well. The red arrow in Figure 22 shows an example of a higher peak caused by the rust or dirt on top of the sample. According to Figure 21 and Figure 22, there is not a significant difference between the welds on conventionally cleaned and laser cleaned samples. Figure 23 and Figure 24 show the two welds

in 3D images with the two different pre-treatments, conventionally cleaned and laser cleaned. The colours indicate the height level.

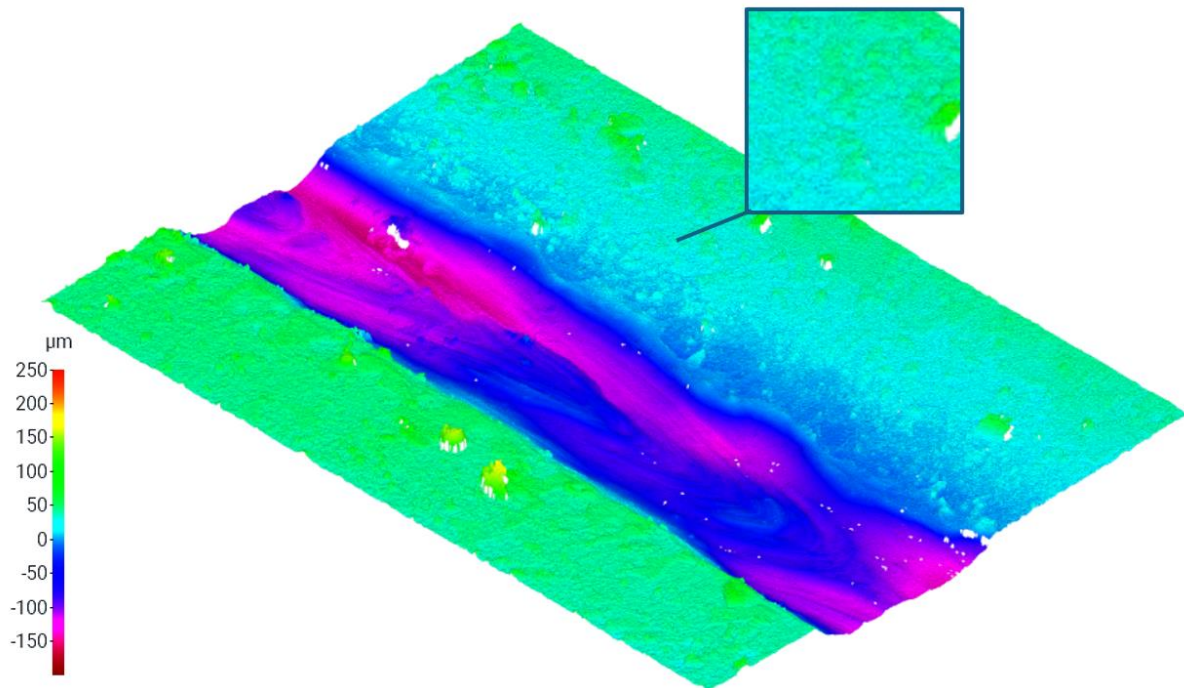


Figure 23. Conventionally cleaned sample surface before welding. The height-colour indicator is on the left.

As shown in Figure 23, the weld can be seen in the middle, the plate is next to the weld on both sides. A height indicator which tells the height by colour can be seen on the left. This tells the height of the sample compared to the reference plane. Some roughness caused by the dirt on top of the surface can be seen next to the weld. The oil and rust is visible as irregularities on the surface. This is also shown on the square which is a closeup of the surface.

The highest peaks are roughly 50 μm higher than the rest of the plain sample, as indicated by the scale in the figure. As shown in the Figure 23, there are some pink-coloured areas in the weld. This means that the weld has sunken almost -150 μm from the top of the plane. The overall figure is similar to the laser cleaned sample in Figure 24, but some differences can be seen.

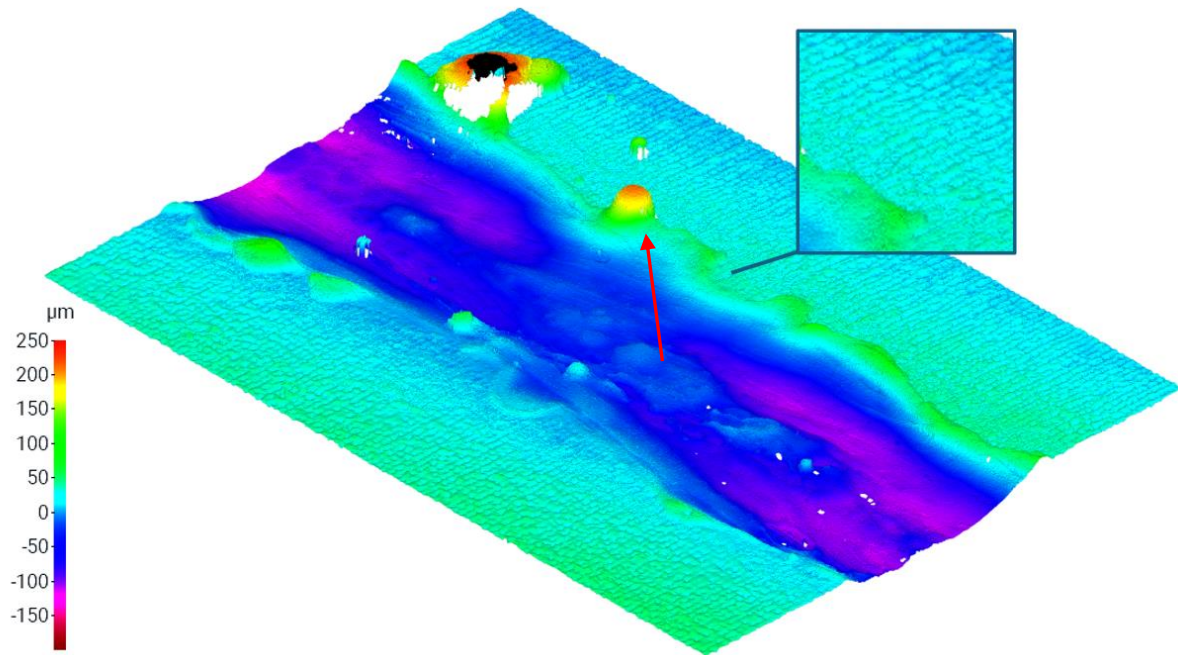


Figure 24. Laser cleaned sample surface before welding. The height-colour indicator is on the left.

As shown in Figure 24, the weld is in the middle of the sample with the plates next to it on both sides. The height indicator which tells the height by colour is on the left. The weld in the middle is lower compared to the plates next to it. The sides of the weld have some spatter and bumps. When compared to the Figure 23, the weld in Figure 24 appears to have less fluctuation in height. The Figure 24 has more even weld as the colour indicates mostly blue with some purple parts.

One of the considerable differences is that the Figure 24 has some higher points (red arrow in Figure 24). Few of the spatters are quite high and reach the height of over 200 μm. These weld spatters were caused by the welding process. The edges of the weld are uneven and raised in some parts. The laser cleaned part next to the weld in both sides have the laser beam path visible. Another difference is the uniform line pattern in the laser cleaned sample, which can be seen in the square on the top right in Figure 24. The roughness of the samples can be seen on Figure 25 and Figure 26.

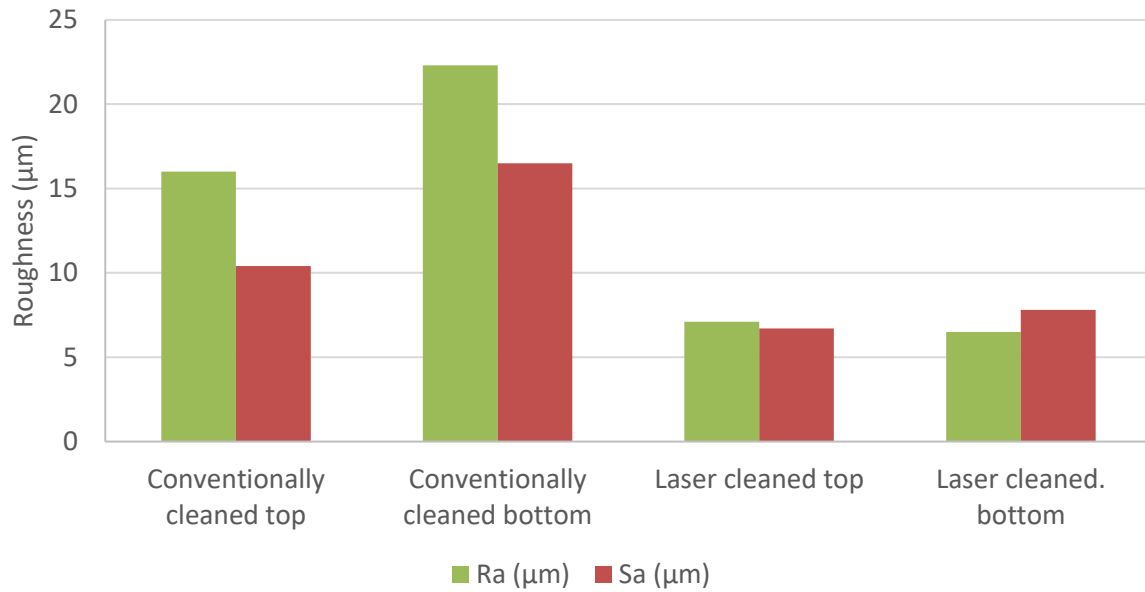


Figure 25. Roughness values Ra and Sa measured from the top of a weld.

As seen on Figure 25, the green columns indicate the Ra roughness values and the red columns Sa values. First two pairs of columns are the conventionally cleaned sample top and bottom values and the latter two are laser cleaned top and bottom sample values. The roughness values are calculated from the weld of the sample to see the cleaning effects on the weld.

The top samples Ra value dropped from 16 µm (conventionally cleaned top sample) to 7.1 µm (laser cleaned top sample), which means that the roughness decreased over 50 %. The Sa values do not have as high decrease, the conventionally cleaned top sample had the Sa value of 10.4 µm and laser cleaned top value 6.7 µm, which is a decrease of 36 %. This may be caused by the uncertainty of calculating Ra values only from a line, as some of the values were not considered when the average roughness was calculated.

A similarity can be seen in both sets of samples. the laser cleaned samples are smoother compared to the conventionally cleaned samples. The Ra for the bottom side of the conventionally cleaned weld is over 22 µm, when the bottom of the laser cleaned sample weld is only about 6 µm, which is about 1/3 of the conventionally cleaned weld. From this can be concluded that the laser cleaning process resulted in a smoother the surface of the weld. However, the difference may be caused by the difference in the weld. The Rz and Sz values for the same samples are shown in Figure 26.

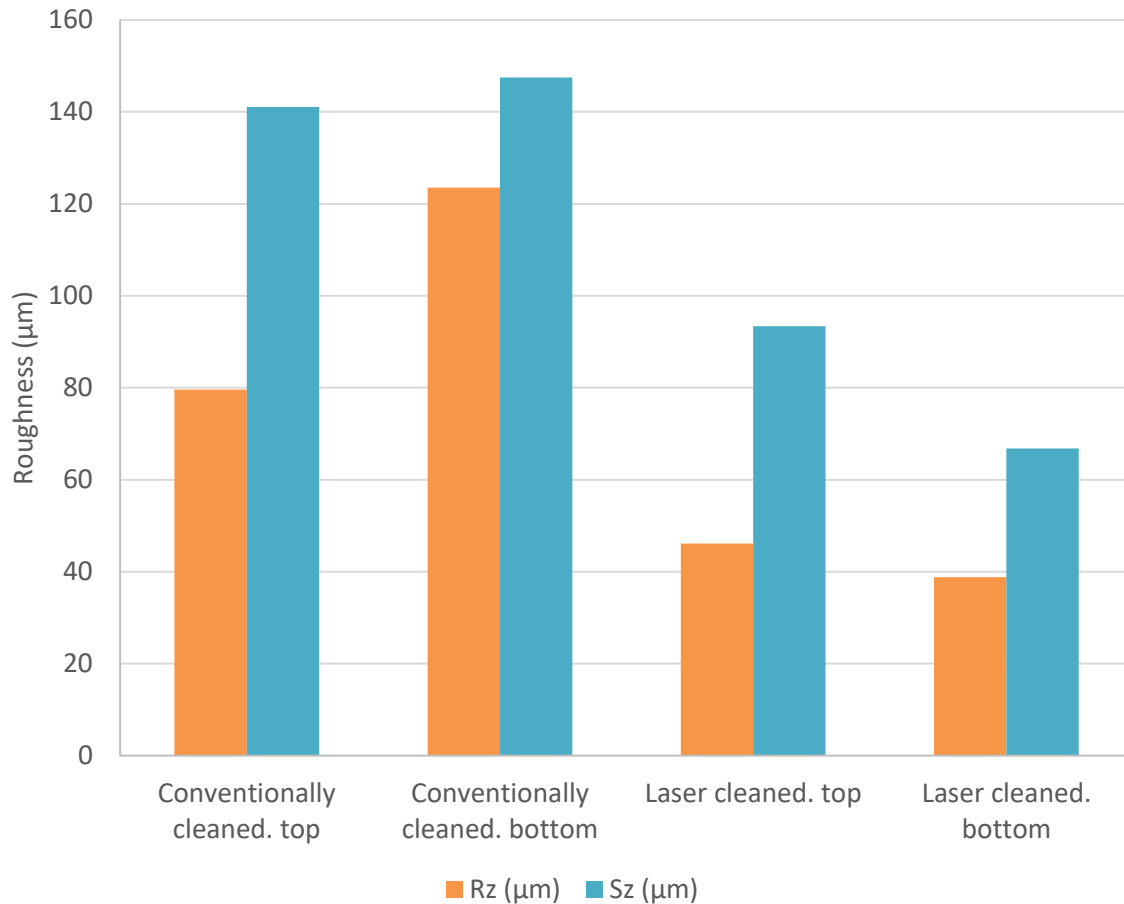


Figure 26. Roughness values Rz and Sz measured from the top of a weld.

As shown on Figure 26, the orange columns indicate the Rz values and blue columns represent the Sz values. The values have been measured from the top of the weld. Again, as was in the Figure 25, the conventionally cleaned samples have higher roughness compared to the laser cleaned samples. It can be concluded that the cleaning was efficient, as some the roughness caused by the dirt has been removed.

The Sz values are higher compared to the Rz values, since the Sz values are calculated from an area, which means that there are more points that are taken into consideration. The Rz values are only taken from a line, which means that some of the highest peaks and lowest valleys may be passed. The non-treated plate and laser cleaned plate without welds were measured to see the roughness differences. This is shown in Figure 27.

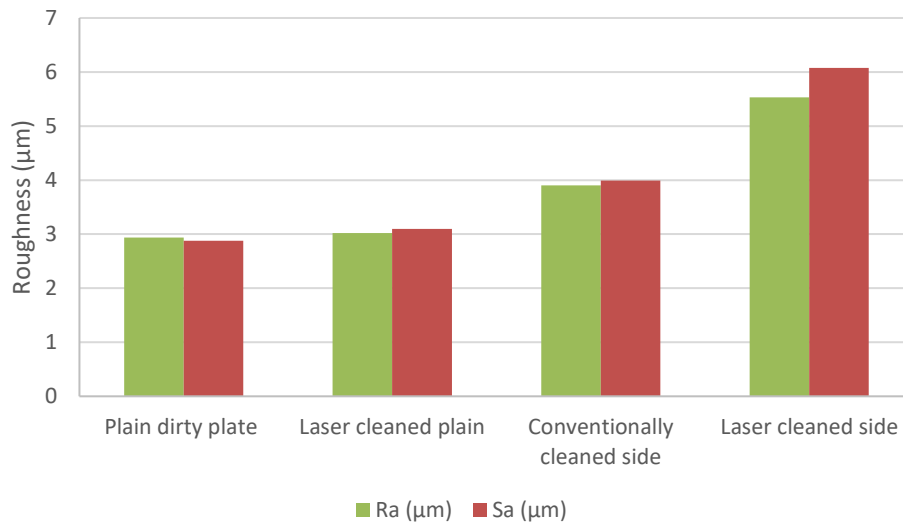


Figure 27. Ra and Sa roughness values for non-treated samples without welds and sides of the sample plates.

As shown in Figure 27 the red columns indicate the Sa values and green the Ra values. The first two values are measured from just the plain sample without any welds. Conventionally cleaned side and laser cleaned side mean the edges which were welded together with same kind of cleaning method.

When the values for non-treated dirty plate and laser cleaned plate are compared, as can be seen from the figure, the values are similar, especially the Ra values. This can mean that the laser cleaning only cleaned the surface without affecting the substrate below it. The dirty plate could have been smooth already without any dirt clumps, so there is not any difference.

Another reason can be that the laser beam was successfully cleaning the higher roughness peaks causing dirt, but the surface pattern creates enough roughness for the surface to not be as smooth as it would have been if only all dirt was removed. When the laser cleaned and conventionally cleaned sides are compared, the laser cleaned is clearly rougher, both Ra and Sa are over 5 µm, when both Ra and Sa for the conventionally cleaned side are around 4 µm. This can be caused by the difference in the sample or because the conventionally cleaning process abraded the larger bumps, when the laser cleaned only removed the dirt from the top of the sample. The Sz and Rz values in Figure 28 are from the same samples as the values from Figure 28.

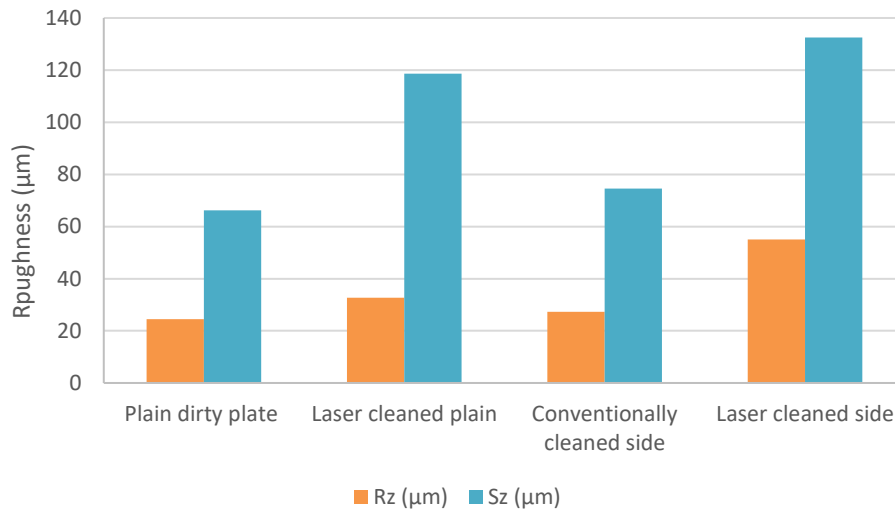


Figure 28. Rz and Sz roughness values for plain and laser cleaned samples and conventionally and laser cleaned sides.

As shown in Figure 28, again the blue columns are the Sz values and orange is Rz. The values for Rz are much lower compared to the Sz values. Some higher peaks and lower valleys have not been taken into consideration when the Rz values were calculated. As the Sz values are calculated from an area, all of the datapoints were included, which is why the columns are much higher.

The laser cleaned side again has higher roughness values compared to the rest of the values. This may be caused the same reason as was discussed before, the cutting may have caused a rougher surface that was slightly polished with the conventional cleaning method.

8.2 Post-treatment (Part 2)

Post-treatment (Part 2a)

Smoothing of the weld was done for the laser cleaned welds.

Figure 29 shows a microscopic image of laser polished sample. This is compared to laser cleaned sample microscope image (Figure 20 from part 1.) as the laser polishing was only done to laser cleaned samples. The scale of the figure is 5 mm which is indicated by the red line in the figure.



Figure 29. A microscope image of laser cleaned and laser polished sample. Red line indicates scale, which is 5 mm.

As shown in Figure 29, the weld is in the middle of the figure in a horizontal orientation. The scale is located in the bottom right corner. The dark area is the laser polished area. The most noticeable difference between Figure 20 and Figure 29 is that as shown in the Figure 29, the laser polished area seems much darker. This however is caused by the reflective properties, and in the weld area in the middle of the figure the real surface appearance can be seen. The laser cleaned weld looks to have a ripple or a waviness, that has been eliminated in the laser polished weld.

Both figures have vertical lines in the entire sample. This is caused by the laser beam, since the laser beam path was equal to the direction of the lines. The laser beam has a small diameter, which means that the melt pool is small. If the laser beam diameter would be increased, the melt pool could be larger. With an increased diameter the surface tension could reach a larger area to smoothen. The Figure 30 and Figure 31 show the profiles of the welds in more detail. This vertical line form that was discussed previously cannot be seen in these figures, since the profile is parallel to the lines.

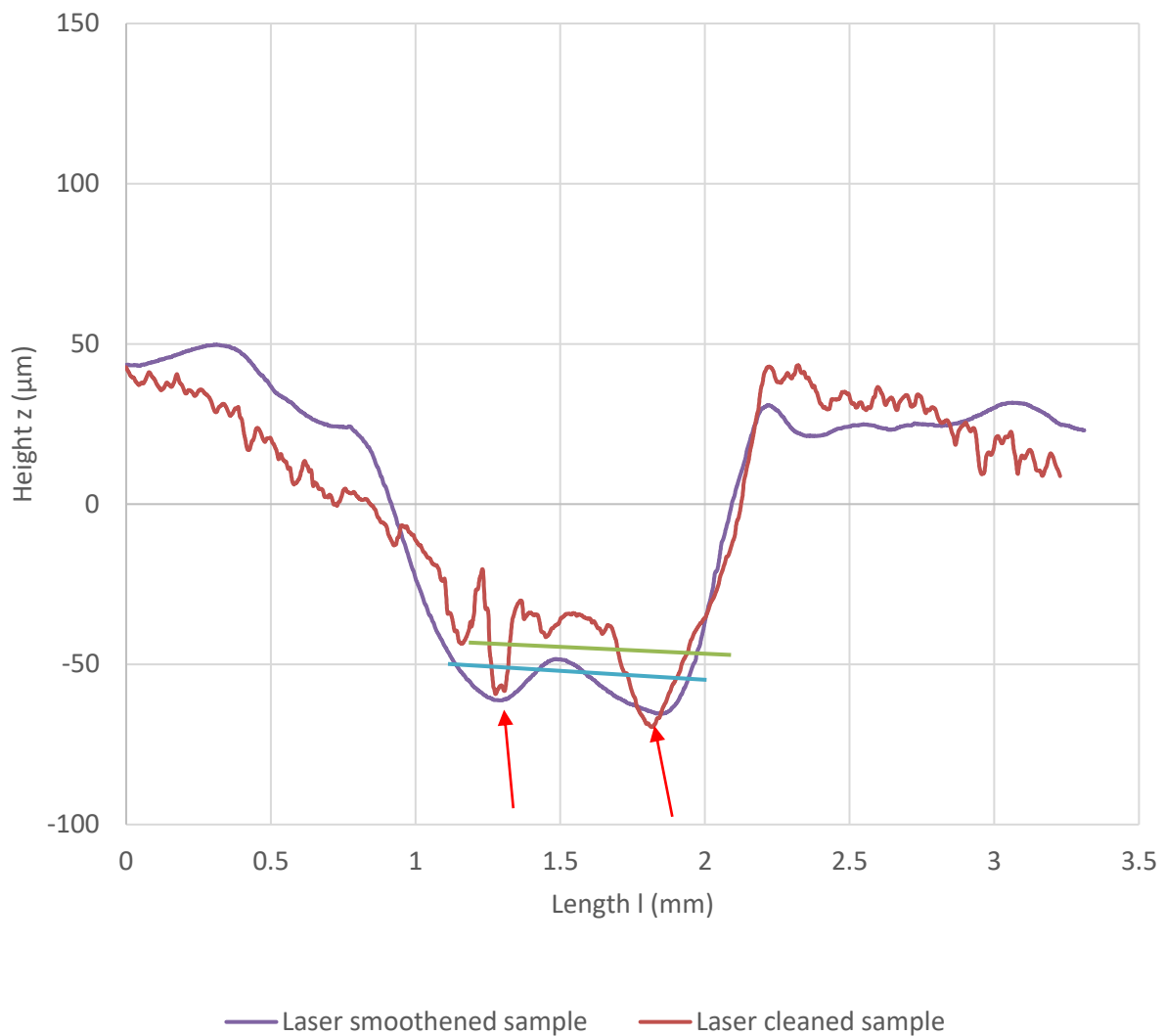


Figure 30. Top side of both laser cleaned (red) and laser polished (purple) profiles. The welds are indicated by green line (laser cleaned before weld) and blue line (laser polished after welding).

As shown in Figure 30, the overall shape for both samples is similar. The red profile shows the profile of the laser cleaned sample weld. The purple profile is the laser polished profile. The blue line indicates the laser polished weld, and the green line laser cleaned weld. Both profiles decrease from the length of 0 mm until 1.25, have a slight increase at 1.5 mm and lowest points at 1.75 mm, with the height of around $-65 \mu\text{m}$. After the low point, the profiles increase steeply to over $40 \mu\text{m}$. The laser cleaned profile decreases from 2.25 mm and laser polished stays roughly the same. The areas around the weld are highly impacted by how the plates were aligned during the welding process.

The most significant difference in the profiles is the lack of roughness in the laser polished profile. Mainly all of the roughness has been smoothed in the laser polished sample, and all

that is left is the form of the surface. The roughness can be seen in the laser cleaned sample as small peaks and valleys with the height of about $5\ \mu\text{m}$. The roughness causes multiple sharper valleys to form. Red arrows point to these. Similarly to Figure 30, Figure 31 has a lot of roughness in the laser cleaned weld profile compared to the laser polished weld profile.

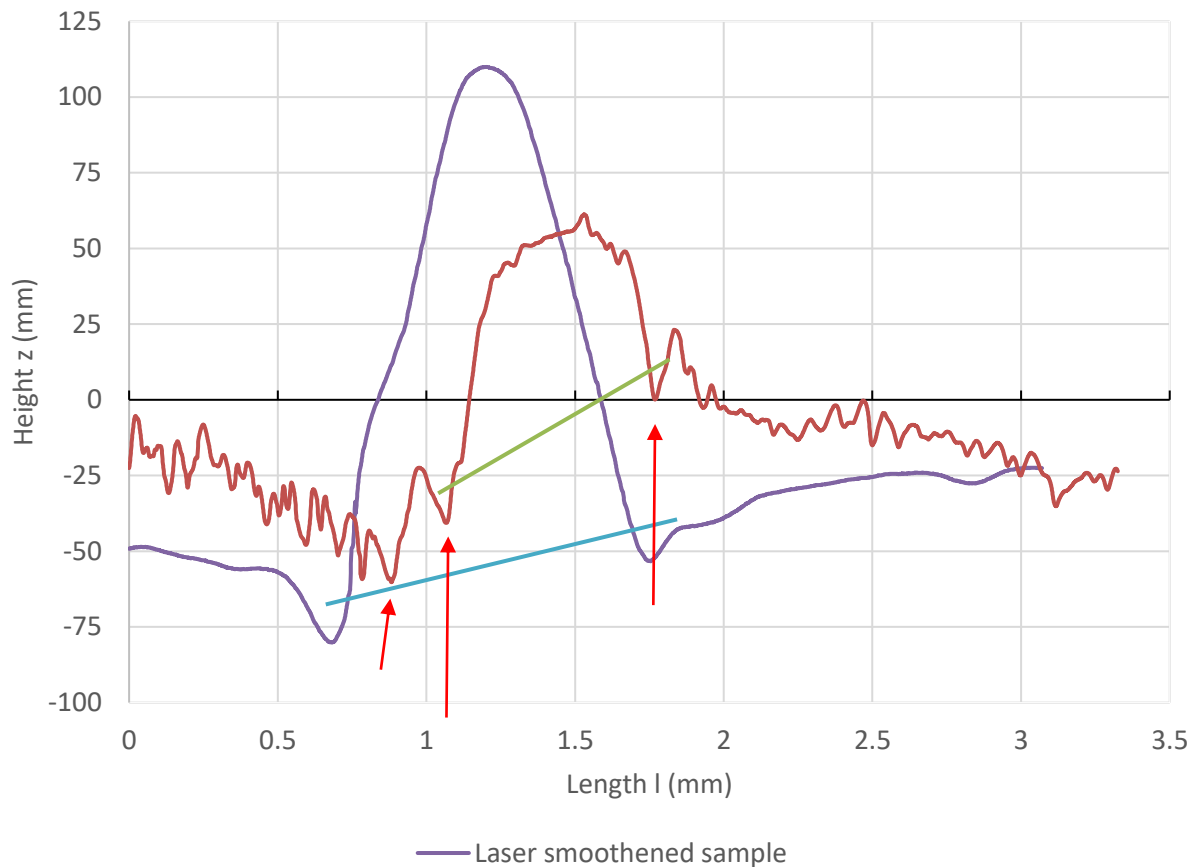


Figure 31. Bottom side of both laser cleaned (red) and laser polished (purple) profiles. The welds are indicated by green line (laser cleaned before weld) and blue line (laser polished after welding).

Figure 31 shows the profiles of the bottom side of the welds. Both profiles first decrease to about 0.75 mm in length. Then the laser polished profile has a high peak, starting from 0.75 mm all the way to 1.75 mm. This peak reaches from the height of $-75\ \mu\text{m}$ to a top height of $110\ \mu\text{m}$ at the length of 1.25 mm. After the top height, the laser polished profile again decreases to the height of $-50\ \mu\text{m}$ at 1.75 mm. The profile slightly increases from 1.75 mm until 3 mm. The peak in the middle of the laser polished profile indicates the weld. This is also shown in the figure as a blue line. The laser cleaned sample profile also has a peak, and the increasing to reach the top starts at the length of 0.85 mm. The highest peak is reached at 1.5 mm with the height of 55

μm . After the peak the laser cleaned profile decreases, between 1.5 mm – 2 mm more steeply, from 55 μm to 0 μm and then between 2 mm – 3.3 mm from 0 μm -25 μm . Again, the angle of the plates is affected by the welding process, and that is why the areas next to the welds do not have completely horizontal trend but decrease or increase.

The laser polished profile in Figure 31 is similar to the laser polished profile in Figure 30 because the laser polishing has eliminated all of the roughness from the surface. There are multiple sharp valleys in the laser cleaned profile when compared to the laser polished profile. The red arrows point to a few of them. These are some of the weakest points if any stresses are focused on or near the weld. The concentration points such as these can be a starting point for cracking and may cause failure of a structure. [47] According to the profiles, these points are eliminated when the weld is laser polished. These experiments would indicate that laser polishing could improve the durability of a weld. As stated, this thesis focuses more on the corrosion and microscopy, which is why it cannot be reliably proven. The methods for researching the mechanical effects on the weld is discussed more in the section Further studies. As stated before, the laser treatment leaves behind a striped pattern, which can be seen in Figure 24 and Figure 32.

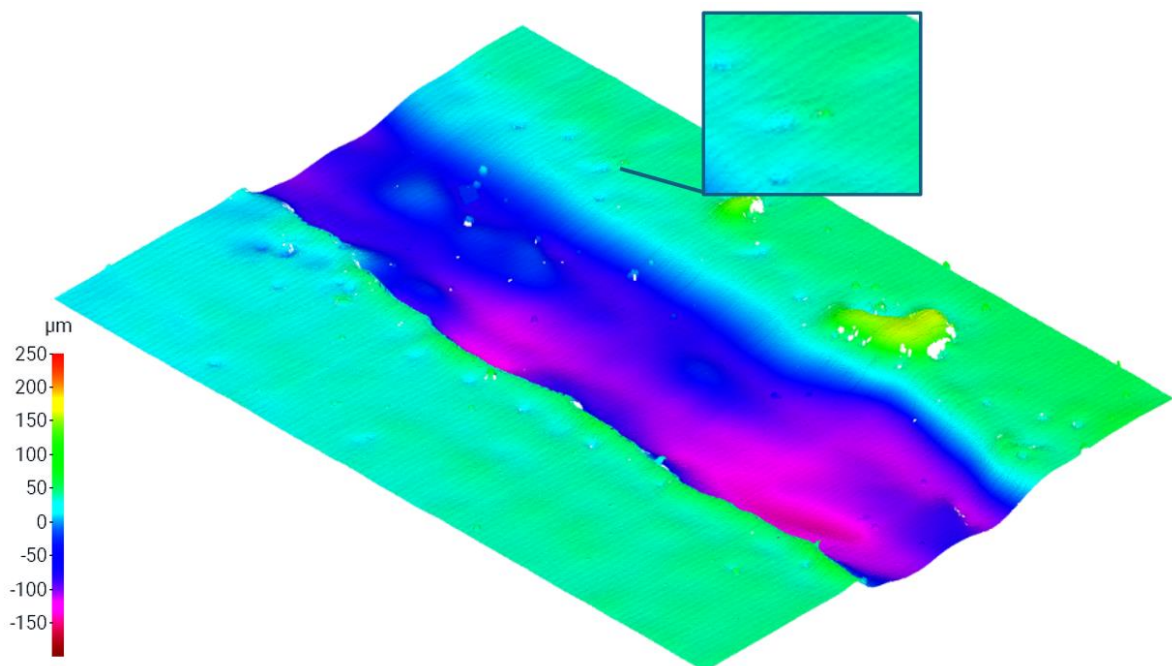


Figure 32. Laser polished sample surface. The height-colour indicator is located on the left.

As shown in Figure 32 the lines are also visible, but not as clearly. It also does not have as many spatters. The few spatters that are visible on the surface are much smoother compared to the spatter in Figure 24. This is also an indication that the laser polishing improves the weld, as spatter is a weld defect [48].

The overall smoother appearance further supports the fact that the concentration points have been eliminated with the laser polishing. According to the height indicator, the weld in the middle (coloured blue) is lower than the bulk material (green). When Figure 32 is compared to Figure 24, the height colours appear to have almost a blurred effect, as the smaller ridges have been able to eliminate and there are no harsher concentration points, especially in the weld. The overall roughness values Ra and Sa can be seen in Figure 33.

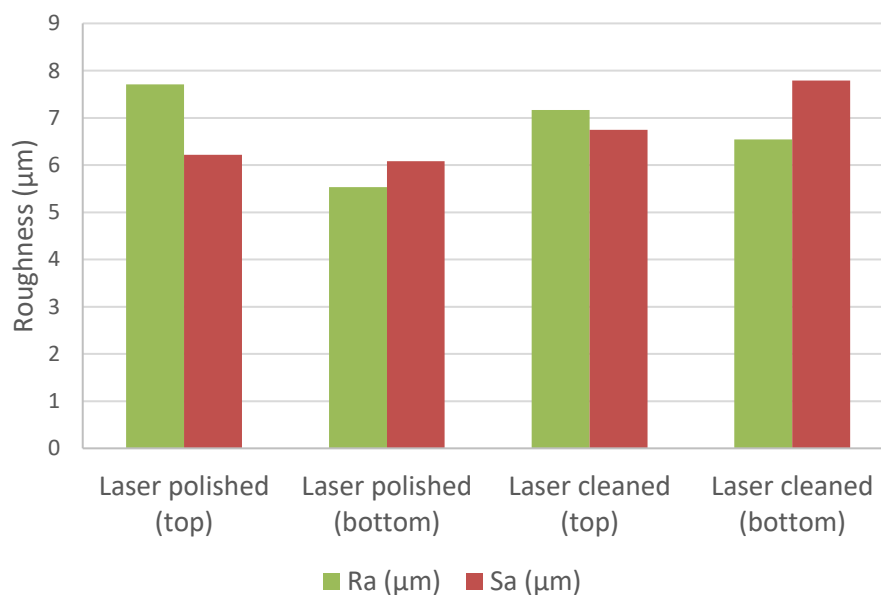


Figure 33. Ra and Sa roughness values of the top and bottom welds.

As shown in Figure 33, the Ra and Sa values are shown as columns. First two column pairs are laser polished samples, and the last two column pairs are the laser cleaned samples. The red columns indicate Sa values and green the Ra values.

The bottom of the weld has improved Ra and Sa values, which means that the surface is slightly smoother compared to the laser cleaned surface. The top side however does not seem to have as much improvement, and in Ra values, the value is higher in laser polishing when compared to laser cleaning values. This can be because of the unpredictability of Ra calculations, since the values taken into account for the Ra calculations can be influenced by the outliers. However,

this effect has been tried to eliminate by selecting multiple Ra values and calculating the average value. The set of values of which the average is calculated should be much larger to reach more accurate values. According to the Sa values, both sides did smoothen, when they were laser polished. The Sa value of laser polished top sample is 7 % lower than the laser cleaned sample. For the bottom samples, the laser polished sample has 22 % lower Sa value compared to the laser cleaned sample. The Rz and Sz values can be seen from Figure 34.

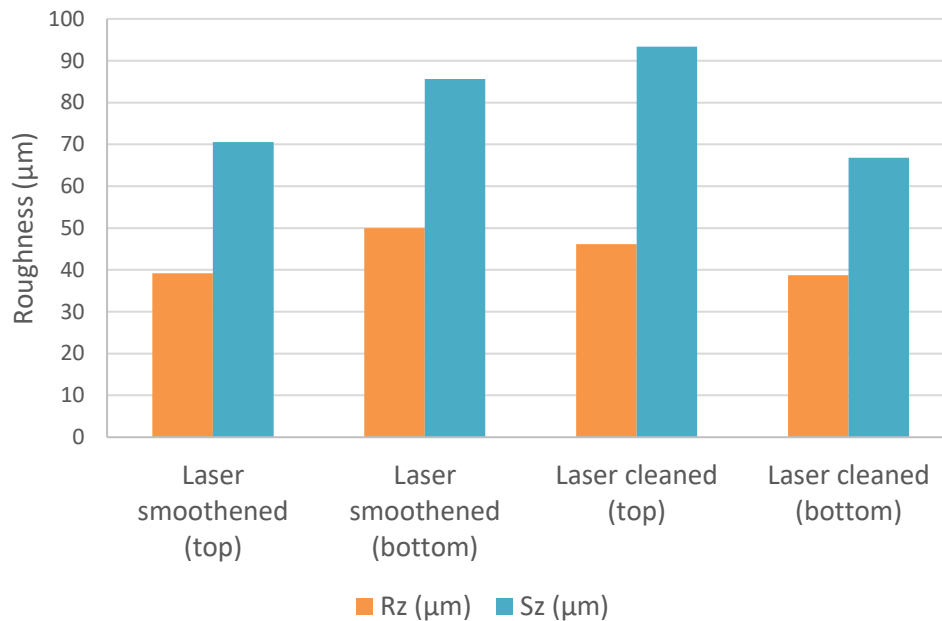


Figure 34. Rz and Sz roughness values of the top and bottom welds.

As shown in Figure 34, the values Rz are indicated by the orange columns and Sz values are the blue columns. First two columns are laser polished samples, and the last two columns are the laser cleaned samples.

The bottom of the laser polished sample has more fluctuation between the lowest and highest point compared to the bottom of the laser cleaned sample, which can be seen from the figure, as the Sz value is higher in the laser polished bottom sample compared to the laser cleaned bottom sample. This can be caused by just the difference in sample, since the sample was different for the laser cleaning process and the laser polishing process. More accuracy could be obtained by first measuring roughness from the laser cleaned surface and afterwards smoothening the same sample. Again, more samples could also be more accurate to calculate the average value of roughness.

Post-treatment (Part 2b)

Another part of the post-treatment was the laser polishing of an additively manufactured surface. Figure 35 shows the surface of the PBF-LB/M sample.

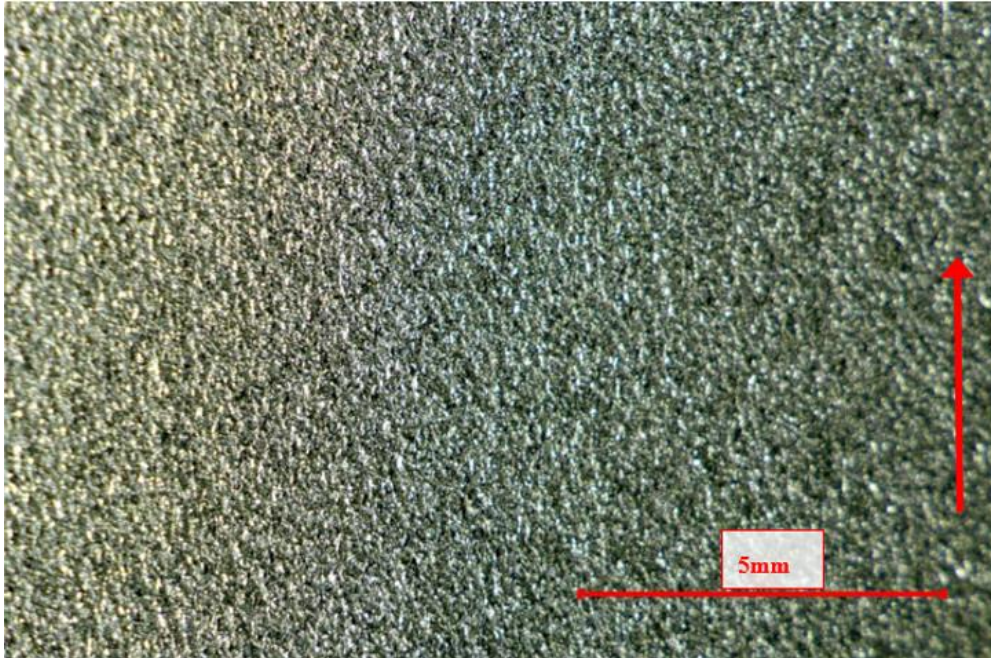


Figure 35. PBF-LB/M surface imaged with a microscope. Scale bar of 5 mm can be seen in lower right corner.

As shown in Figure 35, the surface of the sample is uniform, there are no specific areas where the surface seems to be smoother or rougher. The scale is 5 mm, which means that the irregularity in the surface is quite small. The red arrow indicates the build direction, but the different build layers are not distinguishable from each other. The laser polished sample is shown in Figure 36.

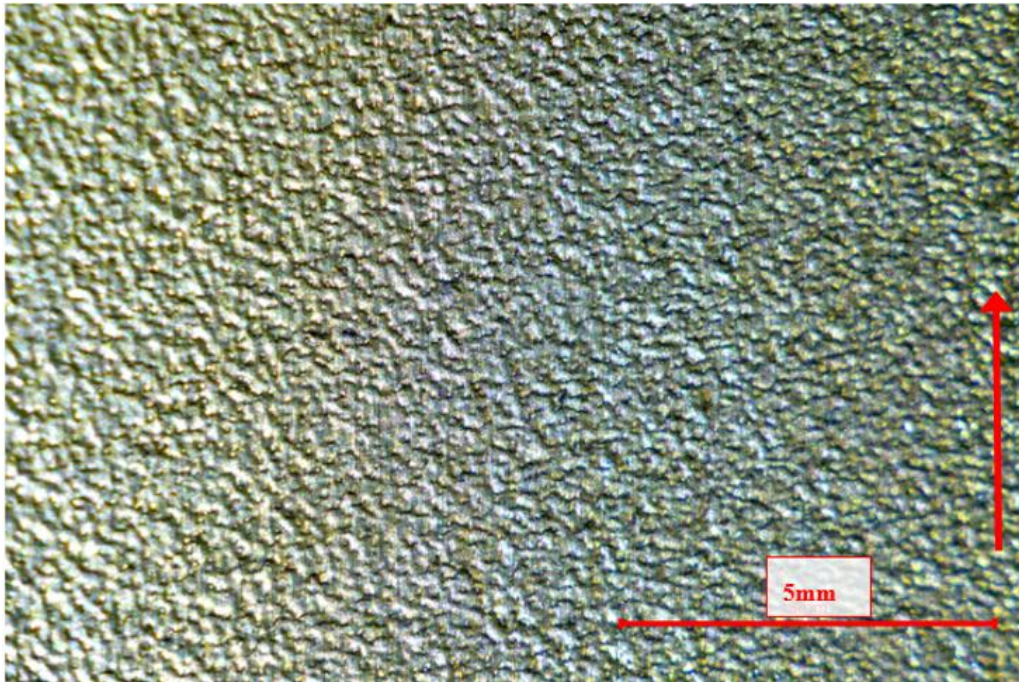


Figure 36. PBF-LB/M laser polished surface imaged with a microscope. Scale bar of 5 mm can be seen in lower right corner.

As shown in Figure 36, the surface is uniform, just like in the sample that was not laser polished. The scale is the same as before, and the build direction is indicated by the red arrow. The overall appearance seems to be smoother as there seems to be fewer irregularities. The size of the irregularities is also larger compared to Figure 35.

Similarly to the laser polished welds, with closer inspection the laser polished PBF-LB/M surface has some vertical lines. These can be assumed to be left from the laser polishing process, as the laser polishing was done parallel to the build direction. The roughness values of the laser polished sample were also measured, and this is shown in Figure 37.

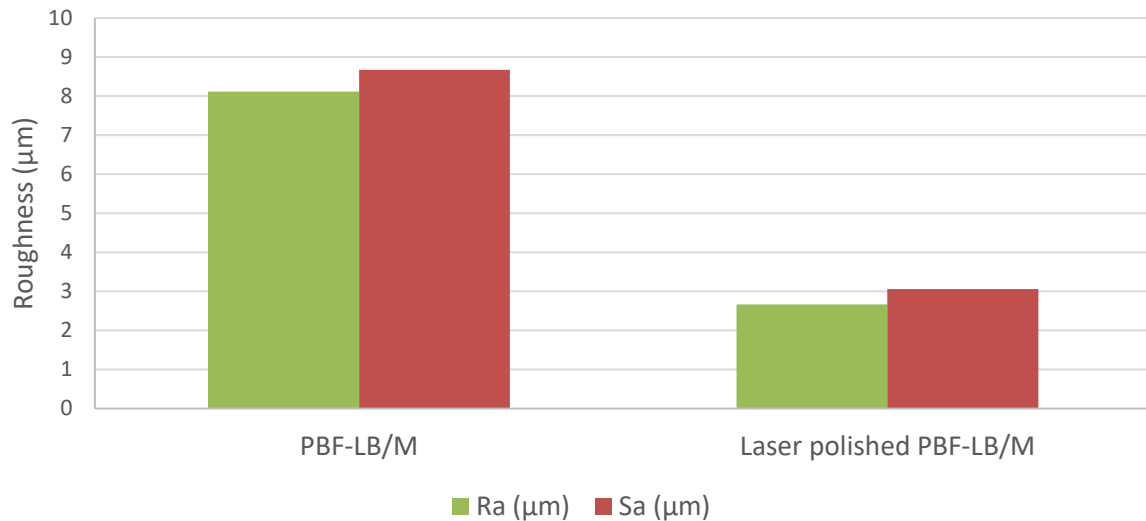


Figure 37. Ra and Sa values for PBF-LB/M and PBF-LB/M laser polished samples.

As shown in Figure 37, the green columns indicate the Ra values, and the red indicate Sa values when the stainless steel. The additively manufactured surface is slightly rougher than all steel parts, but the smoothed sample for PBF-LB/M is significantly improved in smoothness. The Ra and the Sa values are both around three, Ra value being slightly below 3 µm. This means that both Ra and Sa values have the improvement of around 66 %. The Sz and Rz values can be seen in Figure 38.

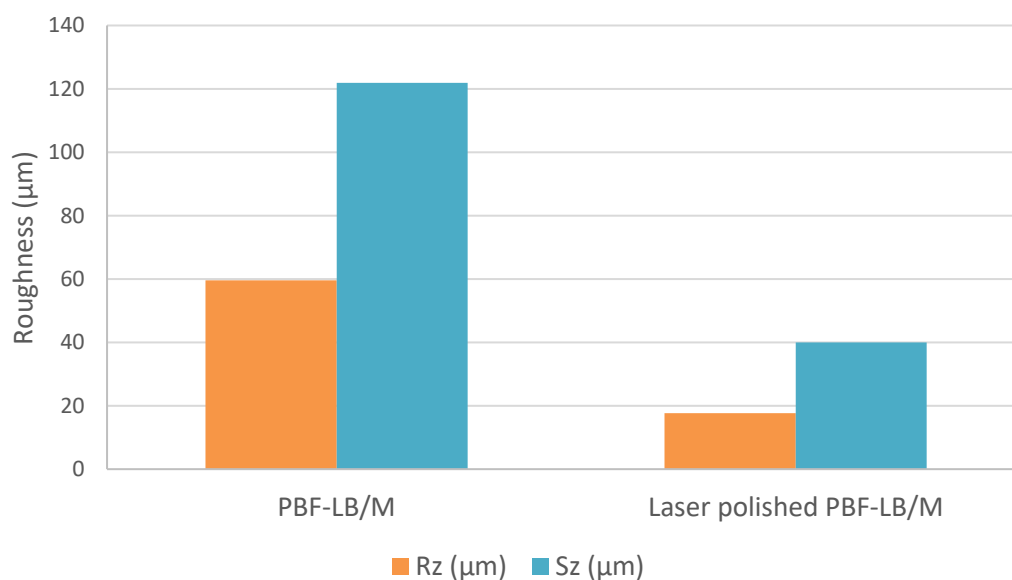


Figure 38. Rz and Sz values for PBF-LB/M and PBF-LB/M laser polished samples.

As shown in Figure 38, the orange columns are the Rz values, blue columns the Sz values. The values are in line with the Ra and Sa values in Figure 37. The laser polished sample has lower values in both Rz and Sz. From this can be deduced that the laser polishing did improve the surface roughness in the additively manufactured sample as the maximum and minimum values have been reduced.

8.3 Corrosion analysis (Part 3)

Corrosion values were measured from all of the samples. The values for the figures can be found from the appendices, Table 11. The E_{corr} values from the non-treated dirty plate and the laser cleaned plain plate can be seen in Figure 39.

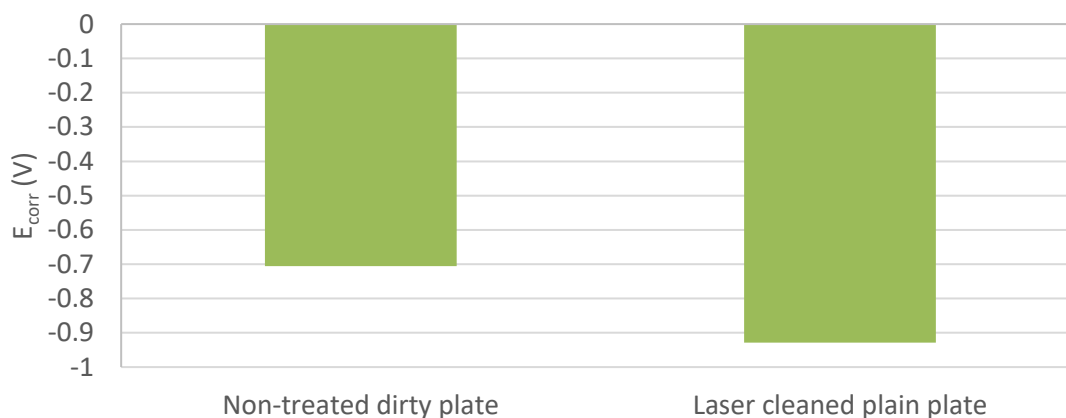


Figure 39. Open circuit potential values for dirty and laser cleaned plate and conventionally cleaned top and bottom of the weld.

As shown in Figure 39, the laser cleaned plate has a lower open circuit potential value, when compared to the non-treated dirty plate. The E_{corr} value for laser cleaned plate is -0.9282, while the dirty plate has E_{corr} value of -0.7053, which means that there is a difference of 31.6 % between the two values. This means that the non-treated dirty plate transfers electrons more easily than the laser cleaned plate and due to this is more likely to corrode faster.

This can be caused by the dirt and oil already on top of the dirty plate. However, this by itself does not tell if the laser cleaned plain plate corrodes faster than the dirty plate. The I_{corr} values for the dirty plate and laser cleaned sample can be seen in Figure 40.

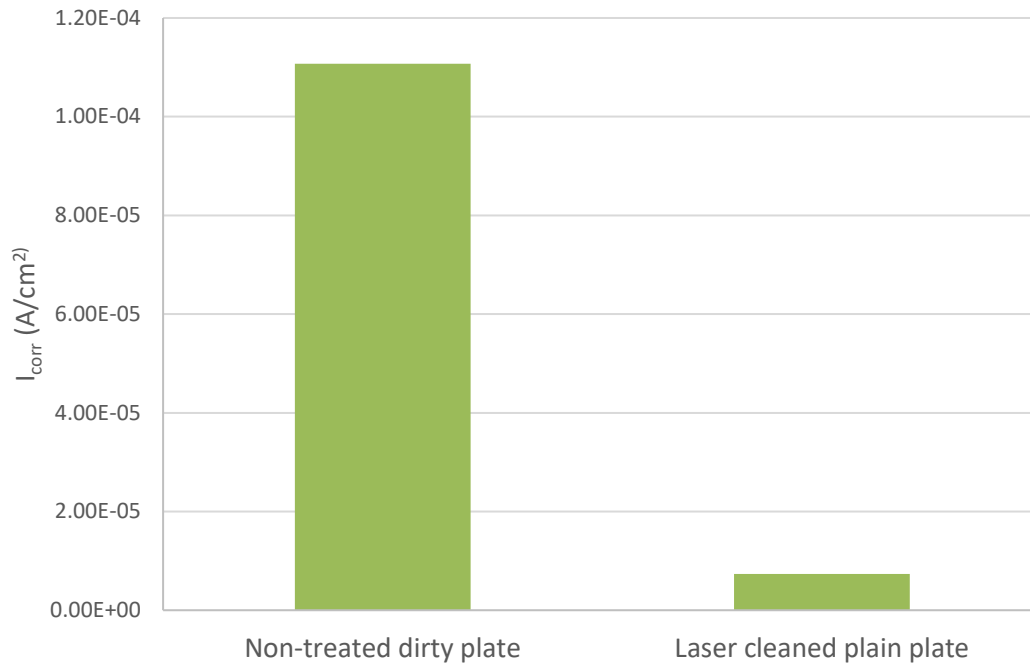


Figure 40. I_{corr} values for plain dirty plate and plain laser cleaned plate.

As shown in Figure 40, the plain dirty plate has a higher I_{corr} value of 1.1×10^{-4} when compared to the laser cleaned sample with the I_{corr} value of 7.4×10^{-6} . Based on this the dirty plate is corroding faster, than the laser cleaned plain plate. One of the reasons can be that the plain dirty plate has some oxidized steel on top of the surface, when the laser cleaned plain plate is dirt free. This means that the non-treated sample is more prone to redox reactions and therefore more prone to corrosion. Corrosion rate is shown in Figure 41.

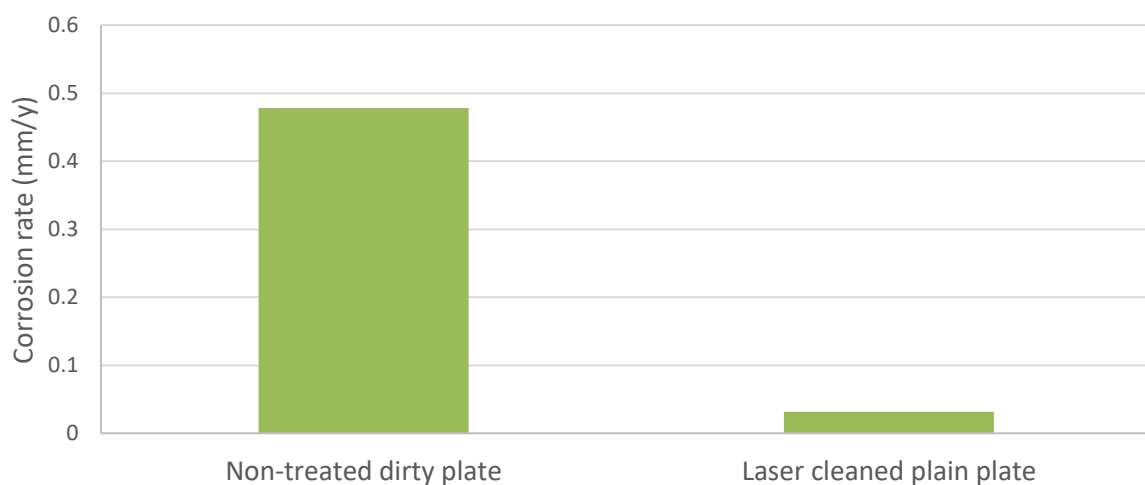


Figure 41. Corrosion rate for plain dirty plate and plain laser cleaned plate.

As shown in Figure 41, the dirty plate has a higher corrosion rate, it corrodes at the rate of 0.4781 mm/y when the laser cleaned plain plate has the corrosion rate of only 0.03178 mm/y. This can again be caused by the oxidation that is already on top of the plate making it dirty. From this it can be concluded that the dirt on top of the dirty plate may be one of the causes why the plate is corroding more compared to the clean sample. The laser cleaning did clean the metal surface, since the corrosion rate is 93.4 % lower in laser cleaned plate than in dirty plate. When considering all three values, E_{corr} , I_{corr} and corrosion rate, the dirty plate appears to be corroding faster, even with the potential being lower.

Pre-treatment (Part 1)

The open circuit potential values for the cleaned samples are shown in Figure 42.

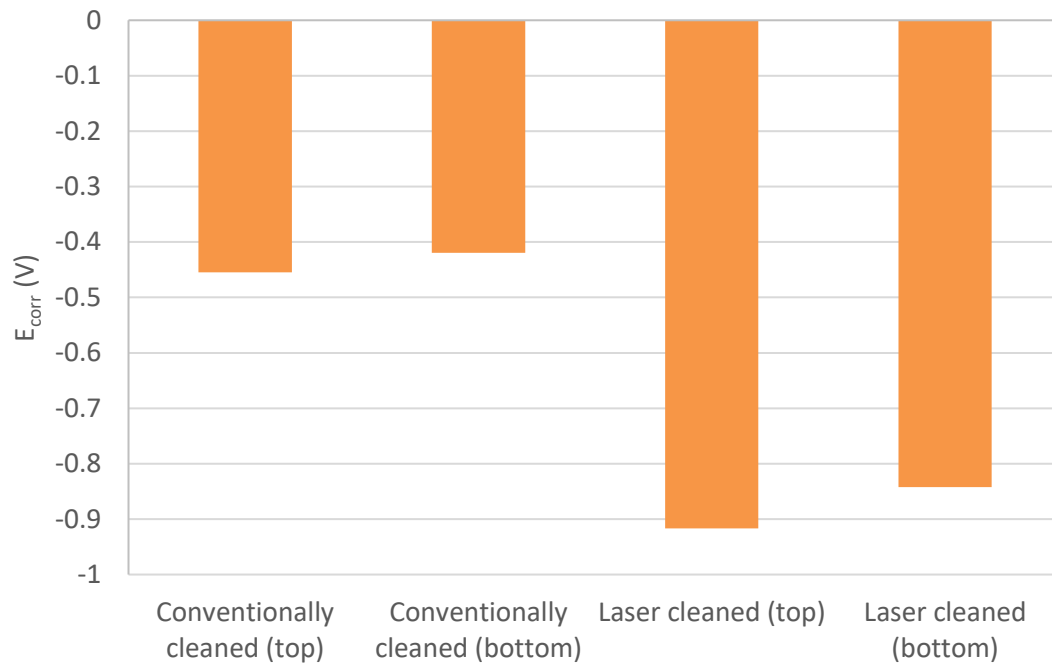


Figure 42. E_{corr} values for conventionally cleaned top and bottom and for laser cleaned top and bottom.

As shown in Figure 42, the conventionally cleaned samples have similarly to the plain dirty plate in Figure 39. The conventionally cleaned samples have the higher open circuit potential compared to the laser cleaned samples. The conventionally cleaned samples are slightly improved from the dirty plate, with the conventionally cleaned top is 55 % higher than the dirty plate and the conventionally cleaned bottom is 68 % higher. This can be caused by the weld, but also the amount of dirt and oil may vary between the different samples.

When compared to the laser cleaned samples, the laser cleaned top has an open circuit potential of -0.917, which is 101,6 % more than the conventionally cleaned top. With the bottom samples, the difference is over 85 %. The conventionally cleaned sample transfers electrons easier, which means that the corrosion should be faster. This may again be caused by the oxidation that has already happened and is on top of the bulk material. The shape of the weld may also have a slight effect on the corrosion properties, as the conventionally cleaned bottom sample have a lower open circuit potential compared to the conventionally cleaned top sample, and the same

happens between the laser cleaned bottom and top samples. The I_{corr} values for the conventionally cleaned and laser cleaned samples are shown in Figure 43.

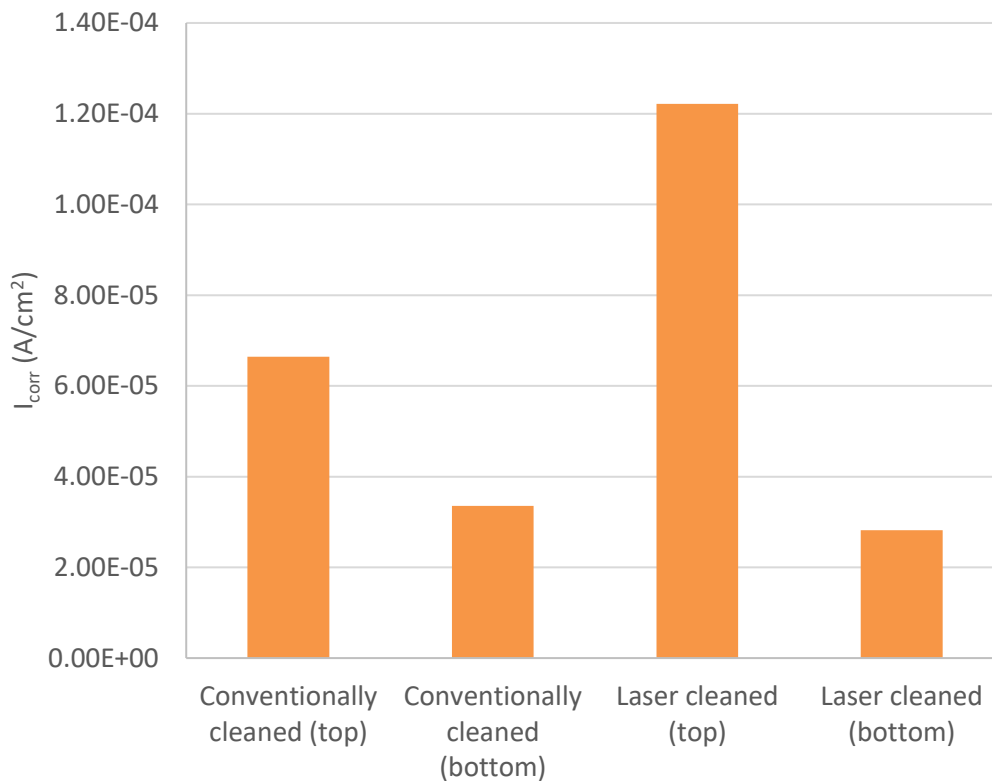


Figure 43. I_{corr} values for conventionally cleaned and laser cleaned top and bottom samples.

As shown in Figure 43, the conventionally cleaned top sample has a lower I_{corr} value than the laser cleaned top. The laser cleaned bottom I_{corr} value is lower than the conventionally cleaned bottom sample. This means that the laser cleaned bottom appears to corrode slower compared to conventionally cleaned bottom, but the laser cleaned top corrodes a lot faster than conventionally cleaned top. The bottom values are more similar to the plates without welds. The reason why the laser cleaned top sample is much higher compared to the rest of the values, especially the laser cleaned top value is unknown. The corrosion rate shows more about the speed of corrosion, and those values are shown in Figure 44.

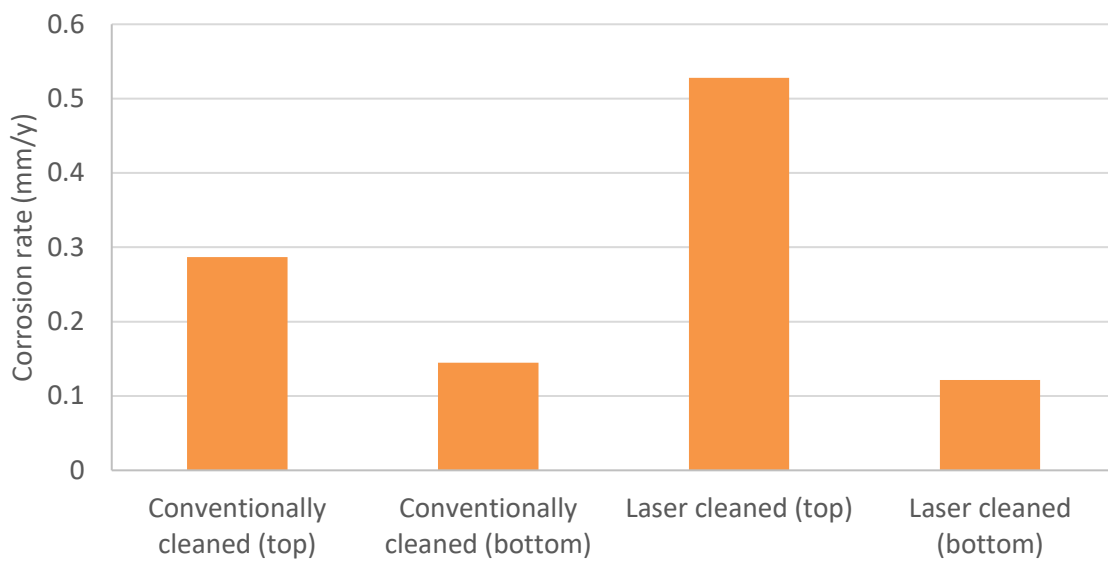


Figure 44. Corrosion rate values for conventionally cleaned and laser cleaned top and bottom samples.

As shown in Figure 44, the values follow the same pattern as with the I_{corr} values. The conventionally cleaned top sample has a lower corrosion rate value of 0.287, than the laser cleaned top where the value is 0.5278. This means that the difference is 45.6%. The laser cleaned bottom corrosion rate value of 0.1217 is 19 % lower than the conventionally cleaned bottom sample that has a value of 0.1449. The difference in laser cleaned bottom and top sample corrosion rates is high, the top sample corrosion rate is over 300 % higher. The reason for this is unknown. There could be a defect in the weld or the laser cleaning was not as effective in the measured spot. The reason for the high laser cleaned top sample value cannot be explained with roughness, since the roughness values were similar in top and bottom of the samples. Further testing should be performed to reach more conclusive results.

Post-treatment (Part 2a)

Laser polishing open circuit potential values are shown in Figure 45.

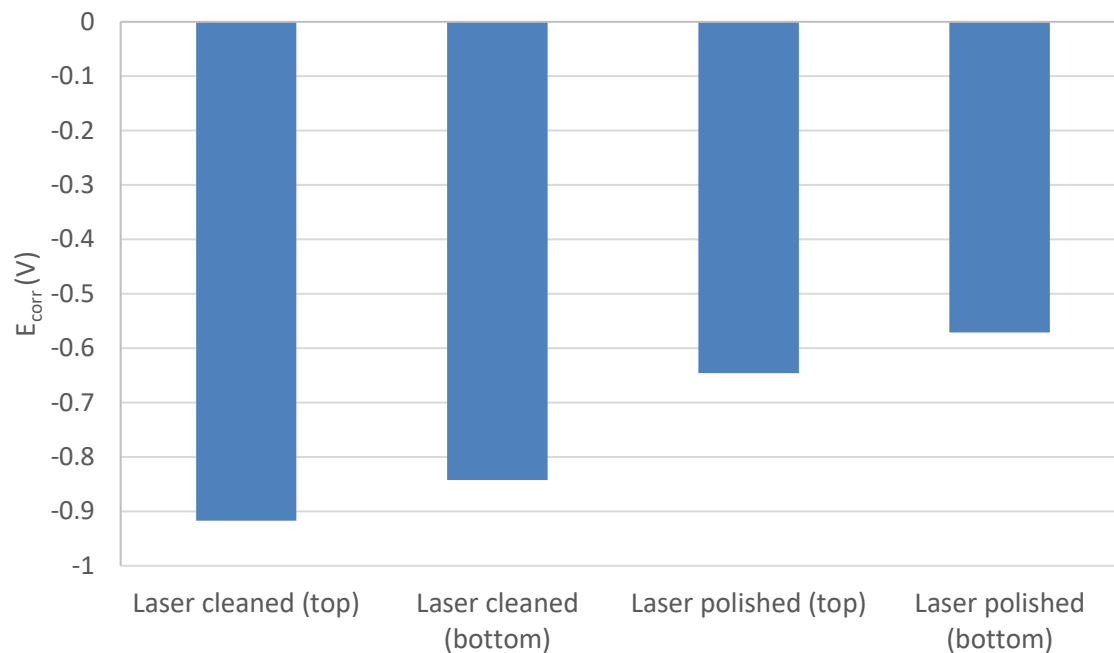


Figure 45. Open circuit potential values for laser cleaned and laser polished top and bottom samples.

As shown in Figure 45, the first two columns for laser cleaned samples have a lower open circuit potential compared to the last two columns for laser polishing samples. The top values have a slightly lower open circuit potential compared to the bottom samples. This means that the laser cleaned samples have a harder electron transfer compared to the laser polished samples.

Both laser polished samples are \pm -0.6 V, which means that it does not reach the open circuit potential of the conventionally cleaned samples or the non-treated dirty plate. The I_{corr} values for the four laser treated samples are shown in Figure 46.

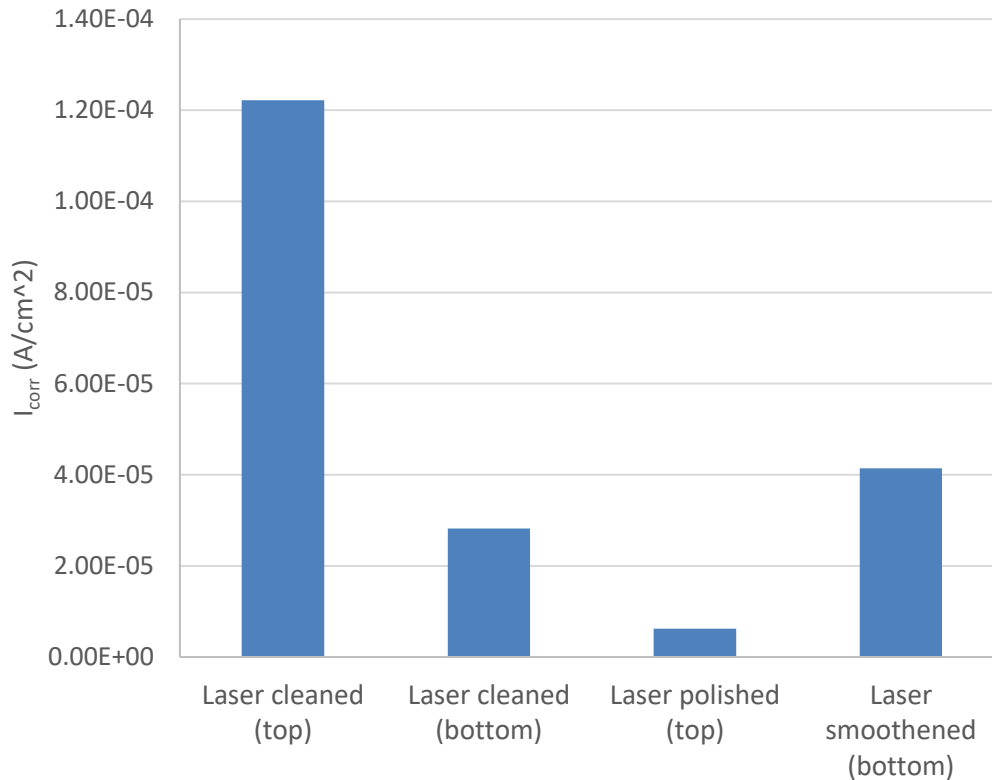


Figure 46. I_{corr} values for laser cleaned and laser polished top and bottom samples.

As shown in Figure 46, the laser cleaned top has the highest I_{corr} value at 1.22×10^{-4} . The lowest value is laser polished top with the value of 6.21×10^{-6} . This means that the difference between the two values is 1816 %. The laser cleaned bottom with the value of 2.82×10^{-5} is lower than laser polished bottom with the value of 4.14×10^{-5} . Some of this may be explained with the differences in samples, and that the laser cleaning process did smoothen the material to some extent. The difference between the two laser cleaned samples is quite large, about 330 %. The difference between the laser polished samples is even larger, about 66 %. The reason for this is unknown. The corrosion rates are shown in Figure 47.

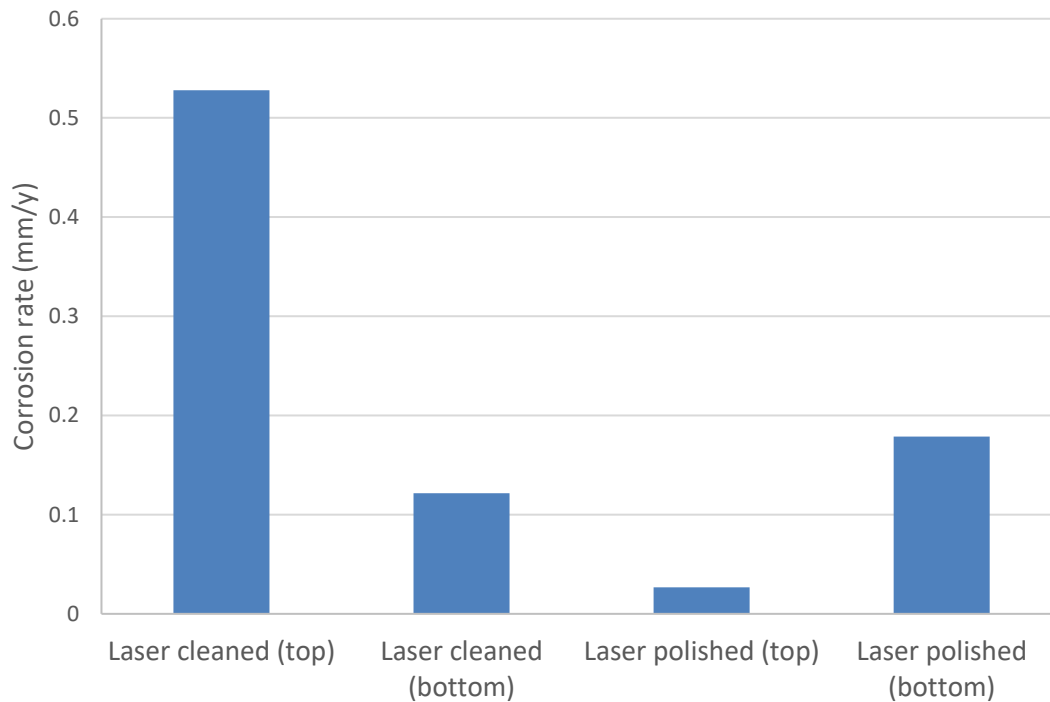


Figure 47. Corrosion rate values for laser cleaned and laser polished top and bottom samples.

As shown in Figure 47, the values again follow the same pattern as with the I_{corr} values in Figure 46. Laser cleaned top sample has the highest corrosion rate and the laser polished top sample has the lowest corrosion rate. Again, the laser cleaned top sample has a lower corrosion rate compared to the laser polished top sample. When the bottom samples are compared, the laser cleaned sample has a lower corrosion rate than the laser polished sample. It is not clear what has caused this. One reason could be that the laser polishing process has oxidized the surface slightly. Another is that the laser polished sample surface has microstructurally changed to a more corrosive type.

If an average is taken from both laser cleaned samples and both laser polished samples, based on that the laser polished samples have lower corrosion rate, as the corrosion rate is lowered 68 %. This is a promising result, as it may protect the weakest points, the welds, even without any coating. This may be caused by the reduction in surface area, as the roughness is removed. However, more data is required to fully conclude that laser polishing does improve the corrosion rate.

Post-treatment (part 2)

The PBF-LB/M samples are separated from the rest of the results due to the difference in material. The open circuit potential values are shown in Figure 48.

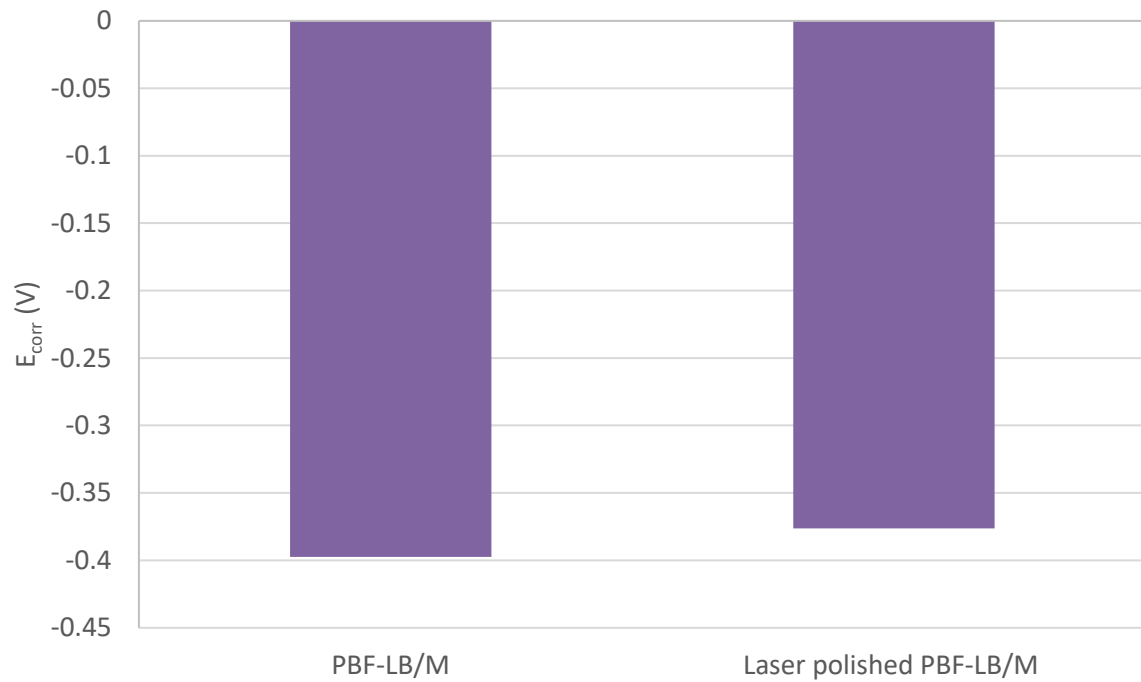


Figure 48. Open current potential values for the PBF-LB/M samples.

As shown in Figure 48, the laser polished sample has lower open circuit potential of -0.376 V, when the open circuit potential for the plain material is -0.398. Overall, the stainless steel has a low open circuit potential when compared to the steel. Based on the previous open circuit potential results and the results on this figure, it can be concluded that the laser polishing does reduce the open circuit potential making the material more prone to electron transfer. This means that the I_{corr} values are shown in Figure 49.

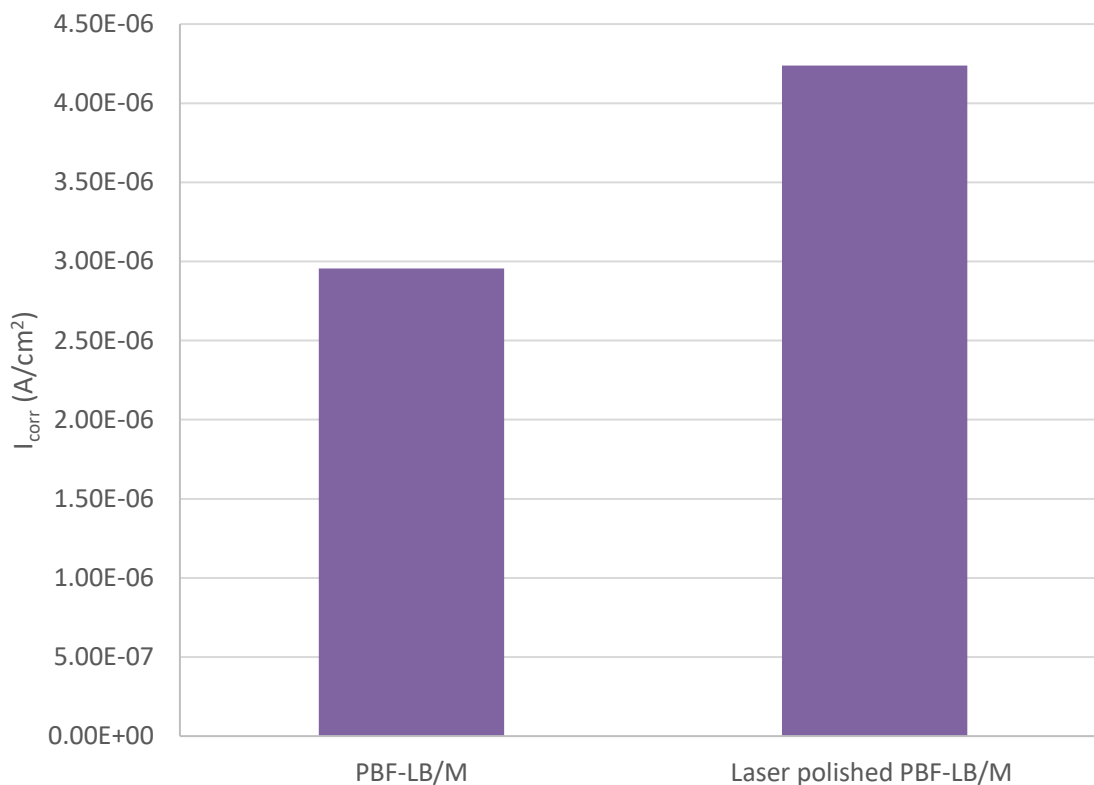


Figure 49. I_{corr} values for plain and laser polished PBF-LB/M samples.

As shown in Figure 49, the laser polished sample has a higher I_{corr} value compared to the plain PBF-LB/M sample. The laser polished sample I_{corr} value is 4.24×10^{-6} A/cm² and the plain is 2.96×10^{-6} A/cm². This means that the difference is 30 %. This figure indicates that the laser polished sample has a higher amount of electrodes involved in the corrosion process. When compared to the open circuit potential, the laser polished should have a lower potential to corrode but according to the I_{corr} value, the laser polished sample should corrode faster. The actual corrosion rate of the material is shown in Figure 50.

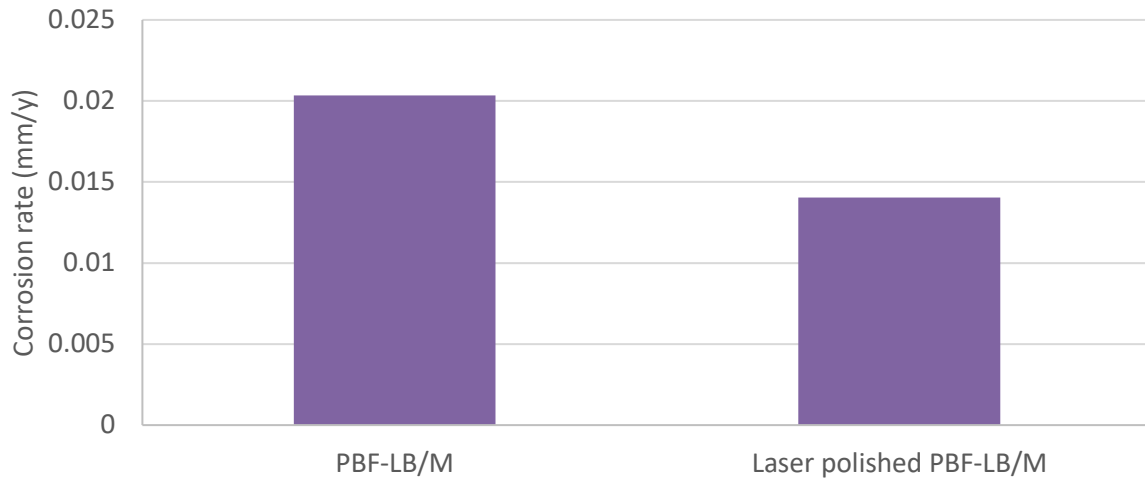


Figure 50 Corrosion rates for plain and laser polished PBF-LB/M sample.

As shown in Figure 50, the corrosion rate is higher in the plain PBF LB/M sample with the value of 0.02 mm/y when compared to the value of the laser polished sample, which is 0.014 mm/y. This would mean that the laser polishing process does reduce the corrosion rate in the PBF LB/M sample.

These results further suggest that the laser polishing should improve the corrosion properties in a material, since the two materials used in this thesis show such improvement. More data could verify the results that were acquired in these results, since there were only a few samples tested. The 316L has the best corrosion rates compared to all samples, but this is due to the material difference.

8.4 Uncertainties

As the research is done with a small sample pool, there are uncertainties that may affect the end results of the thesis. One of the most important uncertainties in this thesis is the cleanliness of the sample. As the samples with the best results for cleanliness were chosen based mostly on visual inspection, it cannot be absolutely certainly said that the parameters chosen for the sample were the best for laser cleaning. An even narrower parameter pool could have been used to narrow down the possible parameters. Multiple sets of parameters could have also been used for the analysing to see how the different parameters react with the testing and analysing.

A similar conclusion can be done with laser polished samples. The parameters were chosen based on what was the smoothest surface in the specific sample pool, and was not investigated further, if parameters near the chosen parameters would have been even better.

The uncertainty of the roughness measurements has been slightly eliminated, as an average was taken from three measurements. However, a difference could be seen if there were dozens of measurements, since the outliers have a much more significant effect on the results with fewer samples. This is a much extensive issue with Ra values, and it has been improved with newer Sa measurements. The Ra measurements were included in this thesis since it still is the more broadly used roughness value. [49] From this it can be assumed that the results achieved are more indicative than exact.

Uncertainties in the corrosion system could be the measurement itself. As all the surfaces were not perfectly smooth, in some cases a few solution droplets were able to escape the beaker during a measurement. Another factor could be that the samples were not measured immediately after cleaning or polishing, and the oil from some samples did slightly rub off the surfaces.

9 Conclusions

The goals for this thesis were to research the possibilities of using a laser cleaning process with a pulsed laser to clean rusted and oily marine grade steel samples before and after welding, and laser polishing the welds to see the effects of the processes in surface roughness and corrosive properties. The experiments were done by using a nanosecond pulsed fibre laser to perform both laser processes. Microscopy with Bruker Alicona G6 was done for surface inspection and roughness analysis and lastly the Ivium electrochemical analyser and Gamry corrosion setup was used to measure corrosion values from the samples.

Literature review from laser cleaning and laser polishing was conducted to research the mechanisms and parameters for the experimental setup. The mechanism of laser cleaning is based on the laser pulse heating the dirt without affecting the substrate below. On a recent research laser cleaning was performed with near-infrared laser (Nd:YAG) with the fluence of 210 mJ/cm^2 and wavelength of 1064 nm . The oil was cleaned from the surface of a carbon steel, stainless steel and copper. The laser cleaned surface had oil which was successfully removed with a $1 \text{ mm} \times 1 \text{ mm}$ square beam. The surface of the substrate melted, when the fluence was over 420 mJ/cm^2 .

Another research about laser cleaning was done with a picosecond pulsed laser Edge Wave PX200-1-GM with a wavelength of 1064 nm and a nanosecond pulsed laser YLP-V2-1-100-100-100 with also a wavelength of 1064 nm . Dirt such as oxide films was cleaned from the surface of an aluminium alloy. The picosecond pulsed laser had the best cleaning results with the average power of 100 W and overlap of 40% . The nanosecond pulsed laser had the best results with the average power of 100 W and overlap of 60% .

Oxidation was also laser cleaned from the surface of a stainless steel. An ytterbium fiber laser was used with the wavelength of 1064 nm and the maximum average power of 15 W . The best results were achieved, with the fluence of 12.4 J/cm^2 and overlap of 80% .

Laser polishing is melting the surface which then smoothens with the surface tension of the melted substrate. It requires less thermal energy compared to laser cleaning. A recent study was conducted with an ultrashort laser pulse laser FX200-1-GF. The laser has a maximum average power P_{ave} of 75 W and wavelength of 1030 nm . The smoothest results were reached with the single pulse peak laser fluence of 0.065 J/cm^2 .

Another research used a prototype of POLAR laser polishing machine. It includes a Yb:YAG disk laser TruMicro 7051 with a maximum power of 550 W and a pulse wavelength of 1030 nm. The best results, the smoothest surface was achieved with the laser fluence of 8 J/cm².

The corrosion is a chemical reaction, where the corroding material, in this case the metal, loses electrons. This means that the structure becomes brittle and may cause failures in the applications. It is a serious challenge especially in the maritime industry.

Samples for the thesis experiments were first cleaned with a laser. A sample was also cleaned conventionally for reference purposes. Multiple parameters were tested, the average power was varied between 25 W – 100 W and the pulse width was varied between 25 ns – 100 ns. The process had the speed of 450 mm/s and pulse frequency of 10 kHz. The laser cleaned areas were visually inspected to select the best parameters that produced the cleanest surface. The best parameters according to this were the average power of 25 W and pulse width of 75 ns.

Secondly the samples were welded and then the weld was laser polished. The same preliminary parameters were used to determine the most melted surface. The best surface smoothness was reached with the average power of 75 W and the pulse width of 25 ns. After both of the laser processes the analysis of the surface and surface roughness measurements were performed with an optical measurement system. Lastly, the corrosion properties were measured with a corrosion setup using a saline solution that complies with standards.

The laser cleaning samples and conventionally cleaned samples did not have any significant differences. The cleaning was successful which can be determined from the microscope images, as the oil and rust is not visible in the laser cleaned samples. The main difference in the welds of the samples is that the laser cleaned weld has much lower roughness values compared to the conventionally cleaned sample. The Sa roughness value in laser cleaned sample is 36 % lower compared to the conventionally cleaned sample. The corrosion rate values were inconclusive with laser cleaned samples and conventionally cleaned samples, as the top conventionally cleaned sample had 45.6 % lower corrosion rate when compared to laser cleaned top sample. However, laser cleaned bottom sample had 19 % lower corrosion rate compared to conventionally cleaned bottom sample.

The laser polishing process smoothed the surface of the sample visually, as the samples seemed to reflect light better compared to the laser cleaned samples. This is visible in the microscope images as the weld of the laser polished sample does not have the same ripple effect that is visible in the laser cleaned sample. The profiles show that the maximum peaks and minimum valleys were removed. This is also visible in the color-indicated figures of the surfaces, as the spatters have been reduced in height. When the laser polished and laser cleaned roughness values are compared, there is not any significant differences. The best improvement was with the Sa values of laser polished bottom sample, which had 22 % lower Sa value compared to the laser cleaned bottom value. The minor improvement could be caused by the ripple effect, which is created by the laser polishing process to the surface of the metal.

The corrosion rates were again inconclusive, as laser cleaned bottom had lower corrosion rate when compared to laser polished bottom sample. However, the laser cleaned top sample had a lot higher corrosion rate compared to laser polished sample. If average from the top and bottom samples is taken, the laser polished sample had 48 % lower than the corrosion rate of laser cleaned sample.

The PBF-LB/M sample was laser polished and the roughness of the sample was lowered 66 % on both Ra and Sa values when compared to the non-laser polished sample. The corrosion rate was reduced 31 % on the laser polished sample, when compared to the non-treated sample. This can be the result of surface area reduction.

Based on the results, the research questions can be answered:

1. The laser cleaning process is a potential way to clean a metal surface, as it does clean effectively without damaging the substrate material below the dirt.
2. Laser cleaning left a smoother weld compared to the conventionally cleaned weld and exhibited better corrosion properties.
3. Laser polishing improves the corrosion resistance of the weld when compared to laser cleaned weld, as the surface area is reduced and high peaks and low valleys are removed.
4. Both the 316L and EH36 behave in a similar way, as the corrosion rate was reduced by laser polishing the surface. Overall the 316L has a lower corrosion rate than the EH36, but this may due to the difference in the alloy.

10 Further studies

Since the topic of the thesis is relatively new, the results were in an experimental level. There are multiple further studies which can be conducted to determine the practicality and reliability of the results that were acquired for this thesis. Multiple studies should be done in the same way and with multiple samples to reach a result that can be said to be more reliable, since this thesis had time restrictions and that could not be done.

Some additional studies can be done to further understand the laser processing effects. One of the studies that can be performed is to use a SEM, where a more detailed analysis can be performed. This method shows the elements that were able to be cleaned with a laser. Other equipment could also be used to inspect the samples to see how the laser treatment changes the microstructure of the metal. This can lead to differences in the properties, such as improve or worsen the hardness on the surface, which will affect the applications where the metal can be used.

Another test that is important when determining the strength of the weld, is tensile testing or similar testing for the ductility. The interest with this specific testing is to conclude if the laser polishing will have any effect on the durability. It was concluded in this thesis that the concentration points were able to be removed, but this does not mean that the structure has been improved. The conventional cleaning method could also be changed with sand blasting, as it is more used in the maritime industry.

When testing the corrosion, the laser polished area can corrode differently when compared to the bulk material. That is why another topic for further studies is to determine the type of corrosion that is happening in the laser polished samples.

References

- [1] A. E. Willner *et al.*, “Optics and Photonics: Key Enabling Technologies,” *Proc. IEEE*, vol. 100, no. Special Centennial Issue, pp. 1604–1643, May 2012, doi: 10.1109/JPROC.2012.2190174.
- [2] *Advances in Laser Materials Processing*. Erscheinungsort nicht ermittelbar: MDPI - Multidisciplinary Digital Publishing Institute, 2022.
- [3] J. P. Davim, “Lasers in Surface Engineering,” in *Laser in Manufacturing*, 1st ed., John Wiley & Sons, Incorporated, 2012, p. 314.
- [4] W. Qiang, G. Yingchun, C. Baoqiang, and Q. Bojin, “Laser cleaning of commercial Al alloy surface for tungsten inert gas welding,” *J. Laser Appl.*, vol. 28, no. 2, p. 022507, May 2016, doi: 10.2351/1.4943909.
- [5] P. E. Lafargue, N. Chaoui, E. Millon, J. F. Muller, H. Derule, and A. Popadenec, “The laser ablation/desorption process used as a new method for cleaning treatment of low carbon steel sheets,” *Surf. Coat. Technol.*, vol. 106, no. 2–3, pp. 268–276, Aug. 1998, doi: 10.1016/S0257-8972(98)00541-6.
- [6] Y. Liu, W. Liu, D. Zhang, Z. Tian, X. Sun, and Z. Wei, “Experimental investigations into cleaning mechanism of ship shell plant surface involved in dry laser cleaning by controlling laser power,” *Appl. Phys. A*, vol. 126, no. 11, p. 866, Nov. 2020, doi: 10.1007/s00339-020-04050-y.
- [7] S. Marimuthu, H. K. Sezer, and A. M. Kamara, “Applications of Laser Cleaning Process in High Value Manufacturing Industries,” in *Developments in Surface Contamination and Cleaning: Applications of Cleaning Techniques*, Elsevier, 2019, pp. 251–288. doi: 10.1016/B978-0-12-815577-6.00007-4.
- [8] J.-E. Kim, M.-K. Song, M.-S. Han, and J.-D. Kim, “A study on the application of laser cleaning process in shipbuilding industries using 100 W fiber laser,” *J. Mech. Sci. Technol.*, vol. 35, no. 4, pp. 1421–1427, Apr. 2021, doi: 10.1007/s12206-021-0113-3.
- [9] D. Ahn, D. Jang, T. Park, and D. Kim, “Laser removal of lubricating oils from metal surfaces,” *Surf. Coat. Technol.*, vol. 206, no. 18, pp. 3751–3757, May 2012, doi: 10.1016/j.surfcoat.2012.03.028.
- [10] G. Koch, J. Varney, N. Thompson, O. Moghissi, M. Gould, and J. Payer, “International Measures of Prevention, Application, and Economics of Corrosion Technologies Study,” NACE International, Houston, Texas, Jan. 2016. Accessed: Sep. 21, 2024. [Online]. Available: <http://impact.nace.org/documents/Nace-International-Report.pdf>
- [11] E. Yasa and J.-P. Kruth, “Microstructural investigation of Selective Laser Melting 316L stainless steel parts exposed to laser re-melting,” *Procedia Eng.*, vol. 19, pp. 389–395, 2011, doi: 10.1016/j.proeng.2011.11.130.
- [12] E. Ukar, A. Lamikiz, L. N. López De Lacalle, D. Del Pozo, and J. L. Arana, “Laser polishing of tool steel with CO₂ laser and high-power diode laser,” *Int. J. Mach. Tools Manuf.*, vol. 50, no. 1, pp. 115–125, Jan. 2010, doi: 10.1016/j.ijmachtools.2009.09.003.
- [13] S. Marimuthu, A. Triantaphyllou, M. Antar, D. Wimpenny, H. Morton, and M. Beard, “Laser polishing of selective laser melted components,” *Int. J. Mach. Tools Manuf.*, vol. 95, pp. 97–104, Aug. 2015, doi: 10.1016/j.ijmachtools.2015.05.002.
- [14] D. Féron, *Marine Corrosion of Stainless Steels*, 1st ed. CRC Press, 2021. doi: 10.1201/9780138748104.
- [15] R. E. Melchers, “Progress in developing realistic corrosion models,” *Struct. Infrastruct. Eng.*, vol. 14, no. 7, pp. 843–853, Jul. 2018, doi: 10.1080/15732479.2018.1436570.
- [16] P. R. Roberge, *Corrosion engineering: principles and practice*. New York: McGraw-Hill, 2008.
- [17] K. De Baere *et al.*, “The influence of concretion on the long-term corrosion rate of steel shipwrecks in the Belgian North Sea,” *Corros. Eng. Sci. Technol.*, vol. 56, no. 1, pp. 71–80, Jan. 2021, doi: 10.1080/1478422X.2020.1807163.
- [18] G. Sun, Z. Wang, Y. Lu, M. Chen, K. Yang, and Z. Ni, “Underwater Laser Welding/Cladding for High-performance Repair of Marine Metal Materials: A Review,” *Chin. J. Mech. Eng.*, vol. 35, no. 1, p. 5, Dec. 2022, doi: 10.1186/s10033-021-00674-0.

- [19] M. Keshavarzan and M. Mohammadi, "A comprehensive metal additive manufacturing platform to transform the marine industry," *MATEC Web Conf.*, vol. 401, p. 02013, 2024, doi: 10.1051/mateconf/202440102013.
- [20] R. W. Revie and H. H. Uhlig, *Corrosion and Corrosion Control - An Introduction to Corrosion Science and Engineering*, 4th ed. USA: Wiley, 2008.
- [21] M. R. Marks, K. Y. Cheong, and Z. Hassan, "A review of laser ablation and dicing of Si wafers," *Precis. Eng.*, vol. 73, pp. 377–408, Jan. 2022, doi: 10.1016/j.precisioneng.2021.10.001.
- [22] X. Li *et al.*, "Influence of ns-Laser Cleaning Parameters on the Removal of the Painted Layer and Selected Properties of the Base Metal," *Materials*, vol. 13, no. 23, p. 5363, Nov. 2020, doi: 10.3390/ma13235363.
- [23] N. B. Dahotre, S. R. Paital, A. N. Samant, and C. Daniel, "Wetting behaviour of laser synthetic surface microtextures on Ti–6Al–4V for bioapplication," *Philos. Trans. R. Soc. Math. Phys. Eng. Sci.*, vol. 368, no. 1917, pp. 1863–1889, Apr. 2010, doi: 10.1098/rsta.2010.0003.
- [24] M. R. Marks, K. Y. Cheong, and Z. Hassan, "A review of laser ablation and dicing of Si wafers," *Precis. Eng.*, vol. 73, pp. 377–408, Jan. 2022, doi: 10.1016/j.precisioneng.2021.10.001.
- [25] E. Assuncao and S. Williams, "Comparison of continuous wave and pulsed wave laser welding effects," *Opt. Lasers Eng.*, vol. 51, no. 6, pp. 674–680, Jun. 2013, doi: 10.1016/j.optlaseng.2013.01.007.
- [26] C. R. Phipps, Ed., *Laser ablation and its applications*. in Springer series in optical sciences, no. 129. New York, N.Y: Springer, 2007.
- [27] G. Zhu *et al.*, "Mechanism and application of laser cleaning: A review," *Opt. Lasers Eng.*, vol. 157, p. 107130, Oct. 2022, doi: 10.1016/j.optlaseng.2022.107130.
- [28] M. Kono, K. G. H. Baldwin, A. Wain, and A. V. Rode, "Treating the Untreatable in Art and Heritage Materials: Ultrafast Laser Cleaning of 'Cloth-of-Gold,'" *Langmuir*, vol. 31, no. 4, pp. 1596–1604, Feb. 2015, doi: 10.1021/la504400h.
- [29] C. Zhou, H. Li, G. Chen, G. Wang, and Z. Shan, "Effect of single pulsed picosecond and 100 nanosecond laser cleaning on surface morphology and welding quality of aluminium alloy," *Opt. Laser Technol.*, vol. 127, p. 106197, Jul. 2020, doi: 10.1016/j.optlastec.2020.106197.
- [30] L. Carvalho, W. Pacquentin, M. Tabarant, A. Semerok, and H. Maskrot, "Metal decontamination by high repetition rate nanosecond fiber laser: Application to oxidized and Eu-contaminated stainless steel," *Appl. Surf. Sci.*, vol. 526, p. 146654, Oct. 2020, doi: 10.1016/j.apsusc.2020.146654.
- [31] S. Nesli and O. Yilmaz, "Surface characteristics of laser polished Ti-6Al-4V parts produced by electron beam melting additive manufacturing process," *Int. J. Adv. Manuf. Technol.*, vol. 114, no. 1–2, pp. 271–289, May 2021, doi: 10.1007/s00170-021-06861-6.
- [32] L. Chen, B. Richter, X. Zhang, X. Ren, and F. E. Pfefferkorn, "Modification of surface characteristics and electrochemical corrosion behavior of laser powder bed fused stainless-steel 316L after laser polishing," *Addit. Manuf.*, vol. 32, p. 101013, Mar. 2020, doi: 10.1016/j.addma.2019.101013.
- [33] M. Chludzinski, R. E. Dos Santos, C. Churiaque, M. Ortega-Iguña, and J. M. Sánchez-Amaya, "Pulsed Laser Welding Applied to Metallic Materials—A Material Approach," *Metals*, vol. 11, no. 4, p. 640, Apr. 2021, doi: 10.3390/met11040640.
- [34] A. Sassmannshausen, A. Brenner, and J. Finger, "Ultrashort pulse laser polishing by continuous surface melting," *J. Mater. Process. Technol.*, vol. 293, p. 117058, Jul. 2021, doi: 10.1016/j.jmatprotec.2021.117058.
- [35] A. Temmler, M. Cortina, I. Ross, M. E. Küpper, and S.-K. Rittinghaus, "Laser Micro Polishing of Tool Steel 1.2379 (AISI D2): Influence of Intensity Distribution, Laser Beam Size, and Fluence on Surface Roughness and Area Rate," *Metals*, vol. 11, no. 9, p. 1445, Sep. 2021, doi: 10.3390/met11091445.
- [36] L. L. Shreir, R. A. Jarman, and Burstein, *Corrosion*, 3rd ed., vol. 1–2, 2 vols. Butterworth Heinemann, 1994.
- [37] N. Nikolov, V. Tsonev, K. Penkov, N. Kuzmanov, and B. Borisov, "Machine for accelerated cyclic corrosion tests through alternate immersion in salt solution," *IOP Conf. Ser. Mater. Sci. Eng.*, vol. 664, no. 1, p. 012016, Oct. 2019, doi: 10.1088/1757-899X/664/1/012016.

- [38] O. Sanni, S. A. Iwarere, and M. O. Daramola, "Introduction: Corrosion basics and corrosion testing," in *Electrochemical and Analytical Techniques for Sustainable Corrosion Monitoring*, Elsevier, 2023, pp. 1–23. doi: 10.1016/B978-0-443-15783-7.00015-3.
- [39] C. Cruz *et al.*, "Effect of Microstructure Features on the Corrosion Behavior of the Sn-2.1 wt%Mg Solder Alloy," *Electron. Mater. Lett.*, vol. 16, no. 3, pp. 276–292, May 2020, doi: 10.1007/s13391-020-00202-7.
- [40] G01 Committee, *Practice for Calculation of Corrosion Rates and Related Information from Electrochemical Measurements*. doi: 10.1520/G0102-89R15E01.
- [41] X. Zou, D. Zhao, J. Sun, C. Wang, and H. Matsuura, "An Integrated Study on the Evolution of Inclusions in EH36 Shipbuilding Steel with Mg Addition: From Casting to Welding," *Metall. Mater. Trans. B*, vol. 49, no. 2, pp. 481–489, Apr. 2018, doi: 10.1007/s11663-017-1163-x.
- [42] S. H. Wang, C. C. Chiang, and S. L. I. Chan, "Effect of initial microstructure on the creep behavior of TMCP EH36 and SM490C steels," *Mater. Sci. Eng. A*, vol. 344, no. 1–2, pp. 288–295, Mar. 2003, doi: 10.1016/S0921-5093(02)00425-2.
- [43] *Hot-rolled steel plates 3 mm thick or above. Tolerances on dimensions and shape*: doi: 10.3403/30156693.
- [44] Electro Optical Systems GmbH, "EOS StainlessSteel 316L Material datasheet."
- [45] Electro Optical Systems GmbH, "Safety data sheet for EOS M 290."
- [46] R. Gao, E. Liu, Y. Zhang, L. Zhu, and Z. Zeng, "Tribocorrosion Behavior of SAF 2205 Duplex Stainless Steel in Artificial Seawater," *J. Mater. Eng. Perform.*, vol. 28, no. 1, pp. 414–422, Jan. 2019, doi: 10.1007/s11665-018-3791-y.
- [47] B. Fuštar, I. Lukačević, and D. Dujmović, "Review of Fatigue Assessment Methods for Welded Steel Structures," *Adv. Civ. Eng.*, vol. 2018, no. 1, p. 3597356, Jan. 2018, doi: 10.1155/2018/3597356.
- [48] K. Omar Cooke and R. Câmara Cozza, Eds., *Engineering Principles - Welding and Residual Stresses*. IntechOpen, 2022. doi: 10.5772/intechopen.96831.
- [49] J. Karlsson, I. Väisänen, E. Tourunen, A. Piironen, A. Gopaluni, and A. Salminen, "Laser polishing of PBF-LB manufactured stainless steel surfaces," *IOP Conf. Ser. Mater. Sci. Eng.*, vol. 1296, no. 1, p. 012023, Dec. 2023, doi: 10.1088/1757-899X/1296/1/012023.

Appendices

Table 9. Preliminary testing parameters for laser cleaning and laser polishing. Green was selected as the laser cleaned sample parameters and orange as laser polished sample parameters.

n	Laser parameters		Laser power W	Pulse diameter mm	Pulse width ns	Pulse frequency kHz	Focal point mm	Treatment rounds	Process speed mm/s
	Fill angle	Fill pitch							
1	0	0.045	25	0.06	25	10	238	1	450
2	0	0.045	50	0.06	25	10	238	1	450
3	0	0.045	75	0.06	25	10	238	1	450
4	0	0.045	100	0.06	25	10	238	1	450
5	0	0.045	25	0.06	50	10	238	1	450
6	0	0.045	50	0.06	50	10	238	1	450
7	0	0.045	75	0.06	50	10	238	1	450
8	0	0.045	100	0.06	50	10	238	1	450
9	0	0.045	25	0.06	75	10	238	1	450
10	0	0.045	50	0.06	75	10	238	1	450
11	0	0.045	75	0.06	75	10	238	1	450
12	0	0.045	100	0.06	75	10	238	1	450
13	0	0.045	25	0.06	100	10	238	1	450
14	0	0.045	50	0.06	100	10	238	1	450
15	0	0.045	75	0.06	100	10	238	1	450
16	0	0.045	100	0.06	100	10	238	1	450

Table 10. Ra, Sa, Rz and Sz values for conventionally cleaned and laser cleaned samples

	Ra (μm)	Rz (μm)	Sa (μm)	Sz (μm)
Conventionally cleaned, bottom	22,3	123,5	16,5	147,5
Conventionally cleaned, top	16,0	79,6	10,4	141,1
Laser cleaned, bottom	6,5	38,8	7,8	66,8
Laser cleaned, top	7,1	46,1	6,7	93,4

Table 11. Corrosion values for all samples

	E_corr (V)	I_corr (A/cm ²)	Corrosion rate (mm/y)
Dirty plate	-0.72	40.5	0.0111
Laser cleaned plate	-0.93	4.58	0.00125
Laser polished weld (top)	-0.64	3.58	0.000979
Laser polished weld (bottom)	-0.57	15.3	0.00419
Laser cleaned with weld (top)	-0.91	55.7	0.0152
Laser cleaned with weld (bottom)	-0.85	10.5	0.00286
Laser polished PBF-LB/M	-0.39	14.8	0.000404
PBF-LB/M	-0.38	11.5	0.000314

Table 12. Parameters for the laser welding.

Parameter	Value
Power	4 W
Process speed	4 mm/s
Focus point	-2 mm